Original Article

MOLECULAR METABOLISM

Beta-hydroxybutyrate counteracts the deleterious effects of a saturated high-fat diet on synaptic AMPAR receptors and cognitive performance

Rocío Rojas[1], Christian Griñán-Ferré[2,3], Aida Castellanos[4,5,6], Ernesto Griego[7], Marc Martínez[1], Juan de Dios Navarro-López[6], Lydia Jiménez-Díaz[6], José Rodríguez-Álvarez[3,7,8], David Soto del Cerro[4,5], Pablo E. Castillo[7,9], Mercè Pallàs[2,3], Núria Casals[1,10,**,11], Rut Fadó[1,8,10,*,11]

ABSTRACT

The ketogenic diet —high in fat and low in carbohydrates— and intermittent fasting have gained popularity not only for weight management but also for their potential to delay cognitive decline associated with neurodegenerative diseases and aging. However, adherence to these diets remains low due to their restrictive nature and undesirable side effects. Both dietary approaches stimulate hepatic production of ketone bodies, primarily β-hydroxybutyrate (BHB), which serves as an alternative energy source for neurons. Here, we investigated whether BHB supplementation could mitigate AMPA receptor trafficking impairments, synaptic dysfunction, and cognitive decline induced by metabolic challenges such as a saturated fat-rich diet. Our results show that, in cultured primary cortical neurons, exposure to palmitic acid decreases surface levels of glutamate GluA1-containing AMPA receptors, whereas unsaturated fatty acids and BHB increase these levels. Furthermore, physiological concentrations of BHB (1—2 mM) countered the adverse effects of palmitic acid on synaptic GluA1 and GluA2 levels in hippocampal neurons, restoring AMPA receptor-mediated synaptic transmission. In hippocampal slices, BHB also reversed palmitate-induced impairments in excitability and synaptic plasticity (long-term potentiation; LTP). Additionally, daily intragastric administration of BHB (100 mg/kg/day for two months) prevented deficits in recognition and spatial memory induced by a saturated fat-rich diet (49% of calories from fat) in mice. In summary, our findings underscore the significant impact of fatty acids and ketone bodies on AMPA receptor abundance, synaptic function, and neuroplasticity, shedding light on the potential use of BHB as a dietary supplement to counteract cognitive impairments linked to metabolic diseases.

Keywords Beta-hydroxybutyrate; Palmitic acid; AMPA receptor; Saturated fatty acid-rich diet; Memory; Synaptic plasticity

1. INTRODUCTION

The escalating prevalence of cognitive impairment and dementia, projected to reach 150 million cases by 2050, represents a severe global public health concern [1]. While increased life expectancy contributes to this outcome, attention has shifted to the impact of nutrition on brain health [2]. Regular consumption of unhealthy saturated fatty acids (SFA), solid fats primarily derived from animals, and trans fats, liquid oils that solidify after food processing, has been associated with impaired memory performance, particularly in both young and old populations [3—5].

During cognitive tasks, neuroplasticity drives the formation and adjustment of synaptic connections, particularly within hippocampal glutamatergic circuits [6]. This process involves dynamic regulation of α-amino-3-hydroxy-5-methyl-4-isoxazolepropionic acid (AMPA)-type glutamate receptors (AMPARs) in the postsynaptic density (PSD).

[1]Basic Sciences Department, Faculty of Medicine and Health Sciences, Universitat Internacional de Catalunya, E-08195, Sant Cugat del Vallès, Spain [2]Department of Pharmacology, Toxicology and Therapeutic Chemistry, School of Pharmacy and Food Sciences, University of Barcelona, Joan XXIII 27-31, 08028, Barcelona, Spain [3]CIBER Enfermedades Neurodegenerativas (CIBERNED), Instituto de Salud Carlos III (ISCIII), Madrid, Spain [4]Laboratory of Neurophysiology, Department of Biomedicine, Faculty of Medicine and Health Sciences, Institute of Neurosciences, University of Barcelona, Barcelona, Spain [5]August Pi i Sunyer Biomedical Research Institute (IDIBAPS), Barcelona, Spain [6]Neurophysiology & Behaviour Laboratory, Regional Centre for Biomedical Research (CRIB), Faculty of Medicine of Ciudad Real, University of Castilla-La Mancha, Ciudad Real, Spain [7]Dominick P. Purpura Department of Neuroscience, Albert Einstein College of Medicine, New York, NY, 10461, USA [8]Institut de Neurociències, Universitat Autònoma de Barcelona, 08193, Bellaterra, Cerdanyola del Vallès, Spain [9]Department of Psychiatry & Behavioral Sciences, Albert Einstein College of Medicine, New York, NY, 10461, USA [10]Centro de Investigación Biomédica en Red de Fisiopatología de la Obesidad y la Nutrición (CIBEROBN), Instituto de Salud Carlos III, E-28029, Madrid, Spain

[11] Núria Casals and Rut Fadó contributed equally to this work.

*Corresponding author. Universitat Internacional de Catalunya, E-08195, Sant Cugat del Valles, Spain. E-mail: rfado@uic.es (R. Fadó).

**Corresponding author. Universitat Internacional de Catalunya, E-08195, Sant Cugat del Valles, Spain. E-mail: ncasals@uic.es (N. Casals).

Received April 14, 2025 • Revision received June 27, 2025 • Accepted July 2, 2025 • Available online 6 July 2025

https://doi.org/10.1016/j.molmet.2025.102207

Glossary

aCSF	artificial cerebrospinal fluid; AMPA
AMPARs	AMPA-type glutamate receptors
AMPA	α-amino-3-hydroxy-5-methyl-4-isoxazole propionic acid
BHB	β-hydroxybutyrate
CD	chow diet
DHA	docosahexaenoic acid
DI	discrimination index
DIV	days *in vitro*
fEPSP	field excitatory postsynaptic potentials
$GABA_A$	γ-aminobutyric acid type A receptor
I/O	input/output
IC	immunocytochemistry
LTP	long-term potentiation
mEPSC	miniature excitatory postsynaptic currents
MUFAs	monounsaturated fatty acids
NMDA	N-methyl-D-aspartate
NORT	Novel Object Recognition Test
OA	oleic acid
OFT	Open Field Test
OLT	Object Location Test
PA	palmitic acid
PM	plasma membrane
PPR	paired-pulse ratio
PSD	postsynaptic density
PUFAs	polyunsaturated fatty acids
SC	Schaffer collateral
SFA	saturated fatty acids
SD	standard deviation
SEM	standard error of mean
SFAD	saturated fatty acid-rich diet
ω-3	omega-3

AMPARs are tetrameric assemblies of GluA1-4 subunits, being the GluA1/GluA2 heterotetramers, that are Ca^{2+}-impermeable, representing the most common arrangement in mature neurons under resting conditions. Upon high neuronal activity, Ca^{2+}-permeable GluA1 homomeric receptors are transiently incorporated into the plasma membrane (PM). This regulated incorporation of GluA1-containing AMPARs supports synaptic potentiation, whereas dysregulation of AMPAR subunit expression or trafficking imbalances can negatively impact synaptic function and cognitive processes [7].

In animal models, diets rich in saturated fatty acids (SFAD) impair memory task performance, particularly in young and aged animals [8–11]. The negative impact of these fats on cognitive function is closely associated with alterations in synaptic function, plasticity, and modifications in synaptic AMPARs [12]. SFAD consumption results in decreased spine density and narrowed PSD in the hippocampus [11], leading to hyper-palmitoylation and hypo-phosphorylation of GluA1 [10]. Treatment with saturated palmitic fatty acid (PA) reduces dendritic arborization and induces synaptic loss in hippocampal neurons, and both effects are effectively prevented when co-treated with the omega-3 (ω-3) docosahexaenoic acid (DHA) [13,14].

Recent evidence suggests that ketogenic diets—characterized by high fat and low carbohydrate content—as well as intermittent fasting, can mitigate cognitive decline associated with aging and neurodegenerative diseases [15]. However, adherence to these dietary interventions is often low due to their restrictive nature, and they are associated with undesirable side effects, such as muscle mass loss, increased total cholesterol and LDL levels, nephrolithiasis, and intestinal discomfort [16,17]. A common feature of both dietary approaches is the induction of hypoglycemia, which subsequently leads to a significant increase in blood ketone body levels (reaching concentrations of 1–5 mM), making them the brain's primary energy substrate [18]. Beta-hydroxybutyrate (BHB) is the most abundant ketone body and has been shown to activate signaling pathways involved in protection against oxidative stress and inflammation [19–22], while also promoting regeneration [23]. These findings suggest that oral supplementation with BHB could represent a promising alternative strategy to mimic the benefits of intermittent fasting and ketogenic diets without the need for strict dietary restrictions. Human studies on ketone supplementation remain limited and report inconsistent results, likely due to high inter-individual variability and small sample sizes [24]. By contrast, although limited in number, preclinical studies have demonstrated some beneficial effects of ketone supplementation in preventing cognitive decline in mouse models of neurodegeneration [25,26]. However, to the best of our knowledge, no studies have yet investigated whether oral ketone supplementation can counteract the detrimental effects of saturated fatty acids on cognitive function and their underlying molecular mechanisms.

In this study, we analyzed the effects of BHB on AMPA receptor trafficking, synaptic function and plasticity, as well as cognitive performance. Our results show that BHB effectively prevents the PA-induced decrease of GluA1 and GluA2 AMPA receptor subunits at both the surface and synaptic levels in cultured neurons. Additionally, BHB counteracted PA-induced reductions in neuronal excitability and synaptic plasticity in hippocampal slices. Importantly, mice fed with a diet high in SFAD, daily intragastric administration of BHB for seven weeks prevented diet-induced cognitive impairments. These findings underscore the therapeutic potential of BHB in mitigating the negative effects of unhealthy dietary fats on brain function.

2. MATERIALS AND METHODS

2.1. Animals and study design

All animal procedures performed at the Universidad de Barcelona were approved by the Local Ethical Committee (#222/18) in accordance with European guidelines (2010/63/EU), while animal procedures at the Albert Einstein College of Medicine were approved by the Institutional Animal Care and Use Committee following the National Institutes of Health guidelines. C57BL/6J mice were housed in a controlled environment with a 12-hour light and 12-hour dark cycle, maintaining consistent temperature and humidity. At five weeks of age, the mice were randomly assigned to one of two dietary groups. One group was fed a chow diet (CD; 10% of kcal from fat and 70% from carbohydrates; D12450J, Research Diets), while the other group received a saturated fatty acid-enriched diet (SFAD) (49% of kcal from fat and 31% from carbohydrates; containing approximately 7% of kcal from palmitic acid; D19121204, Research Diets). The fat sources in the SFAD included soybean oil, high-oleic sunflower oil, flaxseed oil, coconut oil, and butter. In addition, each group was subdivided into two subgroups: one received intragastric administration of D/L-BHB (H6501, Sigma; 100 mg/kg/day) at 8–10 a.m., and the other received an equivalent volume of the vehicle (water). Throughout the study, animals had unrestricted access to food and water. After 7 weeks, the behavioral tests were conducted, and mice were euthanized by decapitation 3 days later, 2 h after the final administration, to collect brain samples. The hippocampus was

preserved for the analysis of protein levels by Western blot, whereas the remaining brain tissue was used to determine BHB levels. To confirm the elevated plasma BHB levels, an additional smaller cohort was fed, administered, and sacrificed 30 min after administration to collect blood samples. Blood and tissue samples were stored at −80 °C for subsequent analysis.

2.2. Primary neuronal cultures

Primary cortical or hippocampal neurons were derived from mouse E16 embryos and obtained as previously described by [27]. Neurons were cultured in plates coated with poly-D-lysine (at 0.05 mg/ml for plastic or 0.1 mg/mL for coverslips; P7886, Sigma) and maintained in Neurobasal medium (21103049, Gibco), supplemented with B27 (17504044, Gibco), glutaMAX (35050061, Gibco), and antibiotics. The cultured neurons were maintained under controlled conditions at 37 °C, 5% CO_2, and 95% humidity. Every 3−4 days, one-fifth of the medium was replaced.

2.3. Cellular treatments

Cortical or hippocampal neurons were treated at 13−14 days *in vitro* (DIV) for 2 or 24 h, as indicated in the figure captions. Stock solutions of 3 mM oleic acid (OA; O7501, Sigma), PA (P9767, Sigma), and DHA (D8768, Sigma) were prepared in defatted BSA solution (0.1 g/mL in 0.9% NaCl), as previously described [28]. Additionally, 250 mM BHB was prepared in water.

2.4. Immunostaining, image acquisition, and analysis

Immunocytochemistry (IC) was conducted on fixed cells using 4% (wt/vol) paraformaldehyde (252549, Sigma) as previously described [29]. For surface GluA1 and GluA2 immunostainings, non-permeabilized cells were directly blocked with goat serum (G9023, Sigma), followed by the primary antibody incubation. The absence of permeabilization was verified by performing an intracellular control staining for the cytoskeletal marker MAP2 (Suppl. Figure 1A). For PSD95, cells were permeabilized using 0.1% Triton X-100 (vol/vol) before blocking and subsequent incubation with the primary antibody. Both mouse anti-GluA1 (1:30; ab174785) and rabbit anti-PSD95 (1:30; ab18258) were obtained from Abcam. Mouse anti-GluA2 (1:30; mab397) was purchased from Millipore. The anti-MAP2 antibody (1:1000; 188002) was obtained from Synaptic Systems. Subsequent incubation was performed with the secondary antibody anti-rabbit Alexa488 (1:300; A11008) and anti-mouse Alexa568 (1:300; A11011), both purchased from Invitrogen. A brief 5-minute incubation with Hoechst solution (1 μg/mL; 14530, Sigma) was performed to visualize cellular nuclei. Finally, coverslips were mounted using Fluoromount Mounting Medium (F4680, Sigma).

Confocal imaging was conducted on immunostained cortical neurons using the Leica DMi8 confocal laser-scanning microscope with a × 63 1.4 NA oil objective. Cells were cultured, stained, and imaged simultaneously using identical settings for quantification. For each condition, 10 randomly selected fields per coverslip and two coverslips per condition were imaged in each experiment. Within each field, 1−2 neurons were assessed, and 1 dendrite per neuron were analyzed. Data were collected from 2 to 3 independent experiments, yielding a total of at least 45 neurons per condition, as detailed in the figure captions. All subsequent quantifications were performed as previously described [29]. The quantification of confocal images was performed on reconstructed 3D images using Imaris 9.2 software (Bitplane). To quantify surface AMPAR levels, primary dendrites, representing the initial branches extending from the cell soma, were selected. Then, a random region of interest (ROI) measuring 15 μm × 5 μm was chosen, and the integrated intensity was measured using the Spot tool in Imaris. To quantify synaptic GluA1 and GluA2 levels, the intensity of GluA1 or GluA2 staining within the 3D ROI defined by PSD95 (used as a synaptic marker) was quantified using the Surface tool in Imaris.

2.5. AMPA-mediated miniature excitatory postsynaptic currents

Miniature excitatory postsynaptic currents (mEPSCs) were conducted in cultured neurons seeded in coverslips, which were mounted in a recording chamber of an inverted microscope (Axio-Vert.A1 Zeiss). Whole−cell patch−clamp currents were recorded at room temperature (25−26 °C) using an Axopatch 200B amplifier−Digidata1440A Series interface board with pClamp10 software (Molecular Devices) as described previously [30]. The extracellular solution used for bathing the cells contained the following (in mM): 140 NaCl, 3.5 KCl, 10 HEPES, 20 glucose, 1.8 CaCl2, and 0.8 MgCl2 (pH 7.4 adjusted with NaOH). To isolate AMPAR-mediated mEPSCs, specific blockers were added to the extracellular solution: 1 μM tetrodotoxin (ab120054, Abcam) to block action potential-dependent neurotransmitter release, 50 μM D-(−)-2-amino-5-phosphonopentanoic acid (ab120003 Abcam) to block N-methyl-D-aspartate (NMDA) receptor and 100 μM picrotoxin (P1675, Sigma) to block gamma-aminobutyric acid ($GABA_A$) receptors. The intracellular solution contained (in mM): 116 K-gluconate, 6 KCl, 8 NaCl, 10 HEPES, 0.2 EGTA, 2 Mg-ATP, 0.3 Na-ATP (pH 7.2 adjusted with KOH). Series resistance was typically 17.71 ± 0.92 MΩ and was monitored throughout the experiment. Cells exhibiting a change in resistance greater than 20% were excluded from the analysis. Data was digitized at 5 KHz and filtered at 2 KHz. mEPSCs were detected using an amplitude threshold of 5 pA. Only events with monotonic fast rise and uncontaminated decay were included. mEPSCs were analyzed with IgorPro 6.06 (WaveMetrics) using NeuroMatic 2.03 [31].

2.6. Hippocampal slice preparation and electrophysiology

Acute slice preparation and electrophysiology recordings were conducted as previously described [32]. One-month-old male mice were deeply anesthetized with isoflurane and then decapitated. The brain was rapidly removed from the skull and submerged in a sucrose-based solution. The sucrose-based solution contained the following composition (in mM): 215 sucrose, 2.5 KCl, 26 $NaHCO_3$, 1.6 NaH_2PO4, 1 $CaCl_2$, 4 MgCl2, 4 $MgSO_4$, and 20 D-glucose. Both hippocampi were carefully dissected. Transverse hippocampal slices (300 μm thick) were obtained by using a vibratome (VT1200s, Leica Microsystems). Then, slices were maintained at 34 °C for 30 min in artificial cerebrospinal fluid (aCSF) continuously bubbled with carbogen (95% O_2/5% CO_2 mixture) and at room temperature for at least 60 min before experimental procedures. aCSF contained the following composition (in mM): 124 NaCl, 2.5 KCl, 26 $NaHCO_3$, 1 NaH_2PO4, 2.5 $CaCl_2$, 1.3 $MgSO_4$, and 10 D-glucose.

Hippocampal slices were placed in an immersion chamber perfused with aCSF (2 mL/min). All experiments were performed at 28 ± 1 °C and in the presence of 50 μM picrotoxin to block $GABA_A$-mediated inhibition. For field excitatory postsynaptic potentials (fEPSP), a stimulating patch-type pipette filled with aCSF and a recording patch-type pipette filled with 1M NaCl were placed in the *stratum radiatum* of CA1 with a distance of ∼100 μm between them. Synaptic responses were elicited by square-wave voltage or current pulses (100 μs pulse width) delivered through a stimulus isolator (Isoflex, AMPI) at 0.05 Hz. To build input/output (I/O) curves, stimuli from 10 to 90 V were used. The paired-pulse ratio (PPR) was calculated as the ratio between the slopes of the second response by the first one. Long-term potentiation (LTP) was induced using a high-frequency stimulation protocol consisting of two trains of 100 pulses, 100 Hz delivered with a 10-second interval

between them. Whole-cell patch-clamp recordings were performed in CA1 pyramidal cells. The patch pipettes were pulled from borosilicate glass (tip resistance 4–7 MΩ) and were filled with a Cs^+-based internal solution with the following composition (in mM): 131 Cs-gluconate, 8 NaCl, 1 $CaCl_2$, 10 EGTA, 10 D-glucose, and 10 HEPES, at pH 7.2 (285–290 mOsm). Series resistance (15–25 MΩ) was monitored throughout all experiments with a −5 mV, 80 ms voltage step, and cells that exhibited a significant change (>20%) were excluded from the analysis. Excitatory postsynaptic currents (EPSCs) were evoked with an extracellular electrode placed in the *stratum radiatum* of CA1 in the presence of picrotoxin (50 μM). AMPAR-mediated EPSCs were recorded at −70 mV. After 5–10 min of recording, the cell was switched to +30 mV to record NMDA receptor-mediated EPSCs. The AMPA/NMDA ratio was calculated by dividing the peak amplitude of AMPA EPSC by NMDA EPSC. Previously, electronic subtraction was performed to remove any residual AMPA component from the recordings conducted at +30 mV. All recordings were performed using a Multi-clamp 700B amplifier (Molecular Devices). Data were acquired at 5 kHz, filtered at 2.4 kHz and analyzed offline using IgorPro 7 (WaveMetrics).

2.7. BHB determination

For BHB determination in plasma, blood was taken 30 min after administration in anti-coagulant-containing tubes, and plasma was separated by centrifugation at 2,000 g for 15 min at 4 °C. For BHB measurement in brain samples, animals were sacrificed 2 h after BHB administration, tissue was weighed for further normalization, homogenized with 4 volumes of cold BHB assay buffer, and centrifuged at 13,000 g for 10 min at 4 °C to remove insoluble material. Samples were deproteinized with a 10 kDa MWCO spin filter (UFC501098, Merck). According to the manufacturer's protocol, BHB levels were measured using a BHB Assay kit (MAK041, Sigma). The amount of BHB present in brain samples was then normalized by the tissue weight.

2.8. Behavior tests

Novel object recognition test (NORT) was used to evaluate short (2 h) and long-term memory (24 h) as described previously by [33]. For NORT a 90o, two-arm, 25 cm-long, and 20 cm-high maze was used. Before the test, mice were individually submitted to a 3-day habituation period in the maze, 10 min daily. On day 4, they were allowed to explore the maze during a 10-minute acquisition trial (habituation phase), examining two identical (in size, shape, and color) novel objects (O1 and O1′) placed at the end of each arm. 2 h later, short-term memory was evaluated with another 10-minute retention trial, where one of the two identical objects was replaced by a novel one (TO). 24 h later, long-term memory was tested again, using a new object (TN) and one used in the previous trial (TO). The exploration time of the novel object (TN) and the exploration time of the old object (TO) were quantified by visualizing video recordings of each trial session. Object exploration was defined as the mouse's nose touching the object or pointing it toward the object at a distance ≤ 2 cm. The cognitive performance was analyzed using the discrimination index (DI) calculated as (TN-TO)/(TN + TO).

Object location test (OLT) was employed to evaluate hippocampus-dependent spatial learning using a box (50 × 50 × 25 cm) with three white and one black walls. The box remained empty the first day, allowing mice to acclimate for 10 min. The following day, two identical 10-cm-high objects were positioned equidistant from each other and the black wall for 10 min. On the last day, one of the objects was relocated in front of the opposite white wall to test spatial memory, quantified as with NORT.

Open field test (OFT) was used to analyze locomotor activity and anxiety-related behaviors as described previously [34]. For OFT, the box (50 × 50 × 25 cm) was divided into central and peripheral zones to facilitate the analysis of the distance traveled. Mice were positioned either at the center or at one of the corners of the open field. After 5 min of exploration time, the distance traveled, time spent in the central zone and periphery, the number of rearings, grooming, and the frequency of defecation and urination were analyzed.

2.9. Statistical analysis

All results are shown as the mean ± standard error (SEM) or standard deviation (SD). Statistical analyses were conducted using the GraphPad Prism 9.0 Software. According to the normality test (Shapiro–Wilk test and D'Agostino and Pearson test), Student's t-test or Mann–Whitney U test were used when comparing only two groups. If multiple groups with different variables were compared, One-way or Two-way analysis of variance (ANOVA) was performed, followed by Bonferroni tests to assess specific group differences.

3. RESULTS

3.1. Effect of fatty acids and BHB on GluA1 surface levels and AMPAR-mediated synaptic transmission in cortical neurons

Given the pivotal role of GluA1 in shaping synaptic function and plasticity, we explored the influence of saturated PA and the major ketone body, BHB, on GluA1 surface levels *in vitro*. Furthermore, the effects of unsaturated fatty acids, OA and DHA, were also analyzed. For this purpose, mouse primary cortical neurons cultured along 13–14 DIV were treated with either PA (200 μM), OA (200 μM), DHA (200 μM), BHB (5 mM), or vehicle (0.6% BSA) in two distinct regimens: a brief exposure lasting 2 h and a prolonged exposure spanning 24 h. Then, we analyzed GluA1 levels on the PM by IC in nonpermeabilized cells using an antibody against its N-terminal extracellular domain.

Exposure of cortical cultures to PA reduced GluA1 levels at the PM (Figure 1A and Supplemental Figure 1B-E), even with a short exposure. In contrast, OA or DHA treatment increased surface GluA1 (Figure 1B–C), with more pronounced effects with a longer exposure. Interestingly, BHB markedly enhanced GluA1 abundance after both the 2 and the 24 h of exposition (Figure 1D). Despite these changes in membrane content, PA and BHB did not affect total GluA1 levels, as determined by Western blot (Suppl. Figure 2), indicating that their effects were restricted to receptor redistribution rather than overall amount. Conversely, OA and DHA induced a reduction in total GluA1 levels 24 h post-treatment, despite the observed increase in surface abundance, suggesting enhanced receptor turnover.

As an alternative experimental model, we also examined the effects of these nutrients in human-derived SH-SY5Y neuroblastoma cells. This cell line can be differentiated into a neuron-like phenotype upon exposition of retinoic acid, which promotes the growth of neurites. In this context, the treatment of differentiated SH-SY5Y with PA, OA, DHA, or BHB for 24 h was able to recapitulate the same effects observed in cultured cortical neurons (Suppl. Figure 3). Therefore, these neuron-like cells are a suitable alternative *in vitro* model for studying the impact of these nutrients, avoiding the use of animals. Altogether, these results confirm a distinct impact of PA, OA, DHA, and BHB on GluA1 surface levels, with long-term treatment eliciting a more potent effect than short-term exposure.

Since PA and BHB exhibited the most significant regulation of surface GluA1, we explored their effects on synaptic transmission by measuring AMPAR-mediated mEPSCs in primary cortical neurons after exposure to these two nutrients. To isolate AMPAR-mEPSCs, D-(−)-2-

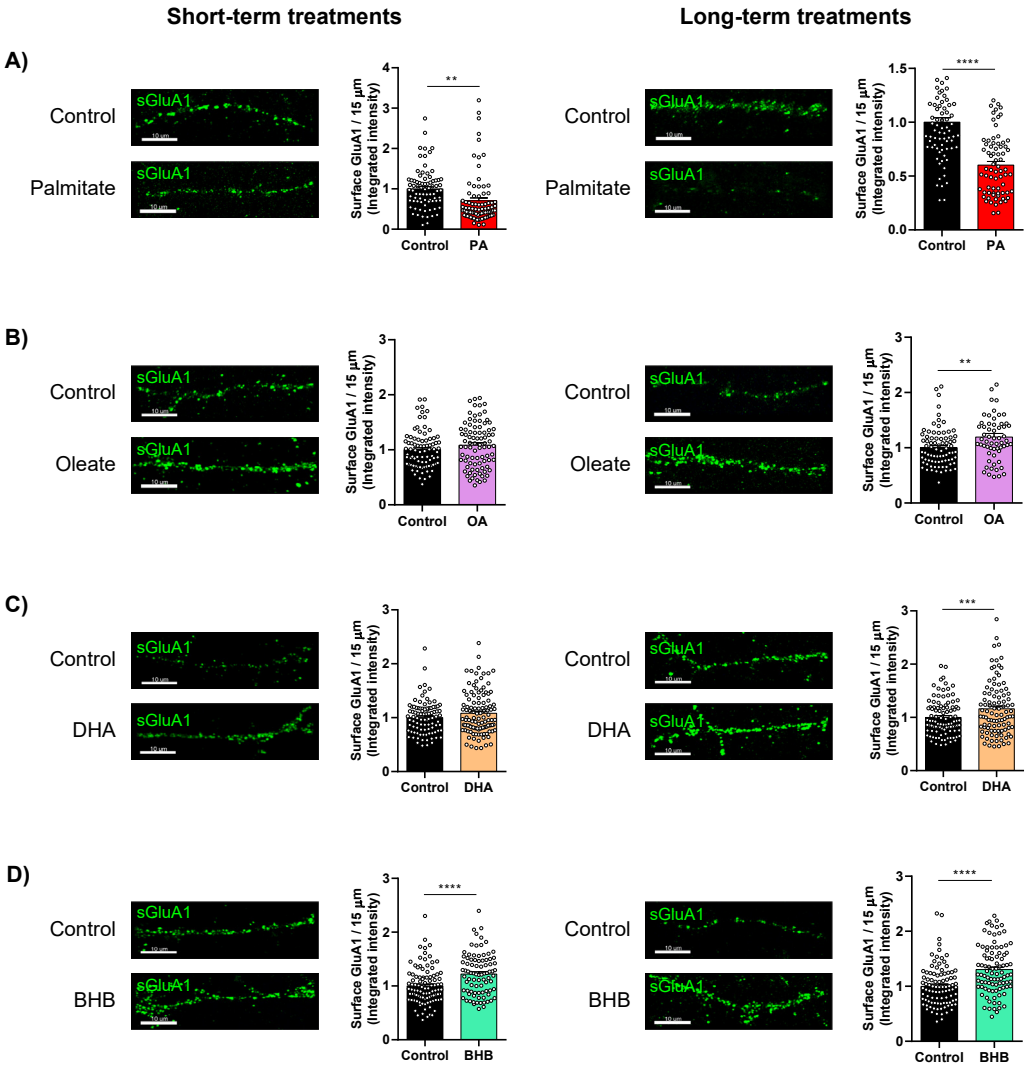

Figure 1: Effects of different nutrients on surface GluA1 levels in primary cortical neurons. Cortical neurons at 13–14 DIV were treated with PA (200 µM; A), OA (200 µM; B), DHA (200 µM; C), or BHB (5 mM; D), respectively. An equivalent volume of vehicle (BSA or water as appropriate) was added to control cells. 2 and 24 h later, neurons were fixed and processed by IC using an anti-GluA1 antibody against the N-terminal domain (extracellular; green stain). Representative images of dendrites are shown (see Supplemental Fig. 1 for complete images). The results in the graphs are the integrated intensity of surface GluA1 normalized by the control given as the mean ± SEM from three independent experiments performed by biological duplicates. (A) Left, control 2 h ($n = 79$ neurons), and PA 2 h ($n = 82$); right, control 24 h ($n = 77$), and PA 24 h ($n = 72$). (B) Left, control 2 h ($n = 84$), and OA 2 h ($n = 86$); left, control 24 h ($n = 80$), and OA 24 h ($n = 60$). (C) Left, control 2 h ($n = 93$), and DHA 2 h ($n = 114$); right, control 24 h ($n = 100$), and DHA 24 h ($n = 99$). (D) Left, control 2 h ($n = 98$), and BHB 2 h ($n = 86$); right, control 24 h ($n = 95$), and BHB 24 h ($n = 93$). **, $P < 0.01$; ***, $P < 0.001$; and ****, $P < 0.0001$. Student t-test. Scale bar = 10 µm. (For interpretation of the references to color in this figure legend, the reader is referred to the Web version of this article.)

amino-5-phosphonopentanoic acid and picrotoxin were added to the perfusion to block NMDA and $GABA_A$ receptors, respectively. The AMPAR-mediated mEPSC amplitude was reduced in cortical neurons treated with PA for 24 h, with no significant changes observed after treatment with BHB (Figure 2A–C). Cumulative amplitude histograms revealed a clear shift in the amplitude distribution towards smaller values under PA treatment (Figure 2D), consistent with a reduction in postsynaptic AMPAR number. In contrast, the frequency of mEPSCs was not significantly affected (Figure 2E), supporting a postsynaptic mechanism. Kinetic parameters such as rise time and τ-weighted were unaffected by these treatments (Figure 2F–G), indicating that the synaptic AMPAR subtype composition remained unchanged. Therefore, exposure to PA decreases the abundance of postsynaptic AMPARs without detectable alterations in their subunit composition. The observation that BHB unaffected mEPSC amplitude and frequency in hippocampal neurons suggests that the increase in surface GluA1 (Figure 1D) might be restricted to non-synaptic regions.

3.2. BHB mitigates palmitate-mediated decrease in synaptic GluA1 levels and restores synaptic transmission in hippocampal neurons

Given the increase of surface GluA1 levels under BHB treatment, we aimed to explore whether BHB could prevent PA-induced synaptic changes, as previous studies have shown that BHB can protect neurons from different types of induced damages [35–37]. To this end, we examined the effects of PA and BHB co-treatment on GluA1 synaptic abundance by colocalizing this receptor with PSD95, a postsynaptic density marker (Figure 1A). Additionally, we tested various concentrations of BHB (1 mM, 2 mM, and 5 mM), which are representative of ketogenic conditions [18], and fall within the upper physiological range of serum BHB levels observed in mice [38]. Here,

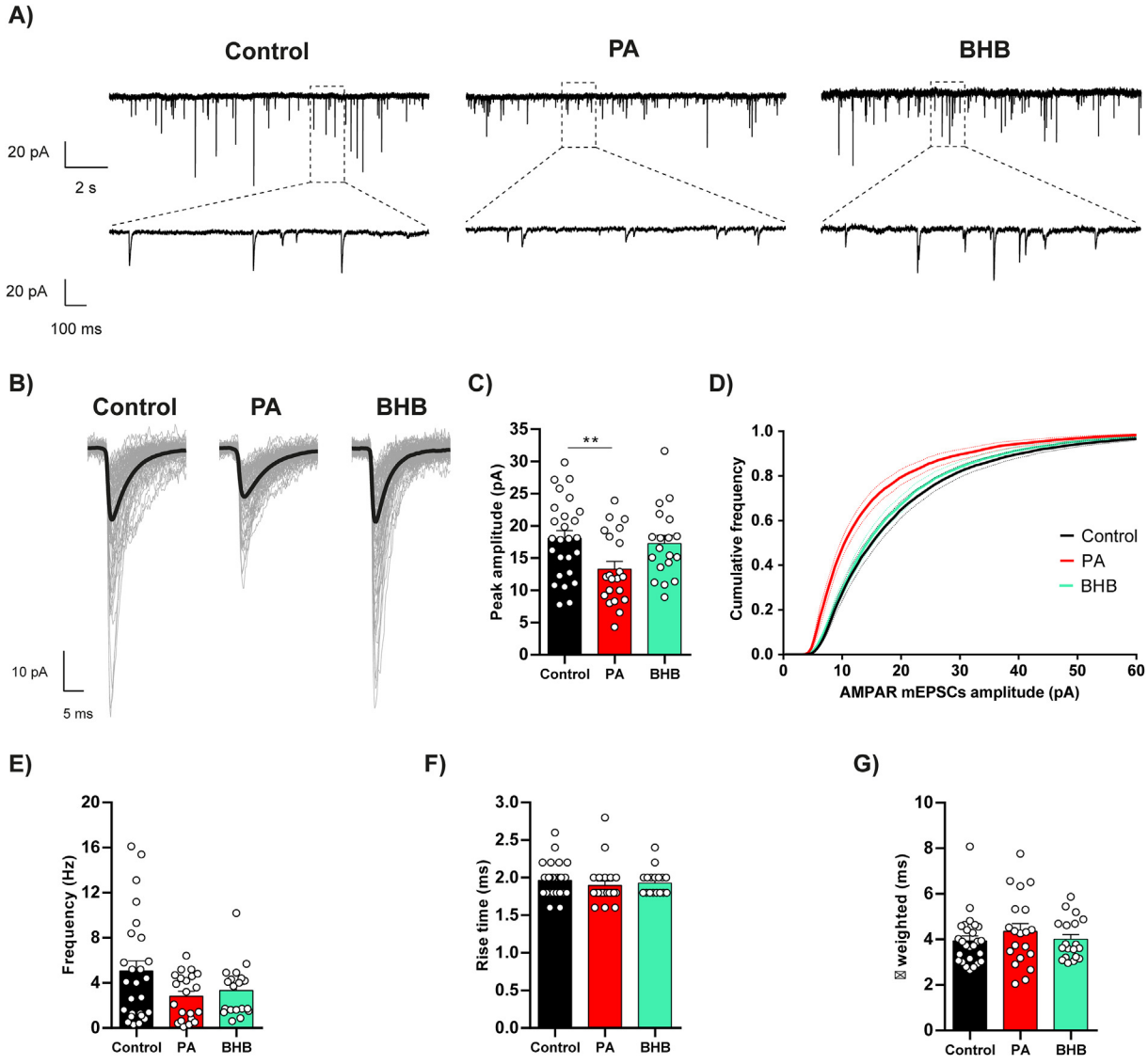

Figure 2: PA and BHB effects on mEPSC in cortical neurons. Cultured neurons at 13–14 DIV were treated with PA (200 μM) or BHB (5 mM) for 24 h. An equivalent volume of vehicle (BSA) was added to control neurons and BHB-treated ones to compare all the conditions properly. (A) Representative traces of AMPAR-mediated mEPSCs. Membrane potential was held at −70 mV. (B) Examples of averaged mEPSCs (bold lines) from 11-, 7- and 5-minutes of time (control, PA, and BHB, respectively) of the recordings shown in A. Control neurons exhibited a mEPSCs amplitude of −18.00 pA (average of 2815 miniature events); PA-treated ones (central traces), −12.10 pA (1967 events); and BHB-treated ones, −18.38 pA (1098 events). One hundred random individual mEPSCs events are shown in grey for each group. (C) AMPAR mEPSCs amplitude was decreased in PA-treated cells compared with control neurons (−18.07 ± 1.20 pA, $n = 26$; −13.28 ± 1.20 pA, $n = 21$; and −17.25 ± 1.27 pA, $n = 19$ cells for each condition). (D) Cumulative probability distribution of mEPSCs amplitude showing a leftward shift in amplitude for events of PA-treated neurons. Continuous lines represent the average for control (black line; $n = 26$ neurons), PA (red line; $n = 21$ neurons), and BHB (green line; $n = 19$ neurons). Thin lines denote the SEM. (E) PA and BHB treatment did not change AMPAR mEPSCs frequency (5.04 ± 0.92 Hz; 2.82 ± 0.44 Hz; and 3.32 ± 0.53 Hz; for control, PA, and BHB, respectively). (F) PA and BHB did not change AMPAR mEPSCs rise time (1.96 ± 0.05 ms; 1.90 ± 0.06 ms; and 1.93 ± 0.04 ms for control, PA, and BHB, respectively). (G) AMPAR mEPSCs τ-weighted was not altered either by PA or by BHB (3.94 ± 0.21 ms; 4.35 ± 0.35 ms; and 4.00 ± 0.21 ms; for control, PA, and BHB, respectively). **, $P < 0.01$. Mann–Whitney test by comparing each condition with the control. (For interpretation of the references to color in this figure legend, the reader is referred to the Web version of this article.)

mouse primary hippocampal cultures were used for two main reasons: first, to determine whether this neuronal type replicates the outcomes observed in cortical cultures; and second, because the regulation of AMPAR number and surface distribution is crucial for long-term synaptic plasticity in the hippocampus, while synaptic plasticity in the cortex is comparatively more restricted [39,40].

As expected, short-term exposition to PA reduced GluA1 surface levels in hippocampal neurons (Figure 3A–B; red bar) and the amount of synaptic GluA1 (Figure 3C; red bar). Moreover, the treatment with PA led to a decrease in PSD95 levels, spot volume, and number of synaptic spots (Figure 3D–E; and Suppl. Figure 4A-B). In contrast, BHB alone did not affect either surface or synaptic GluA1 abundance at any of the tested concentrations, except at 5 mM, which increased surface GluA1 (Figure 3B–C; green bars), as previously observed in cortical neurons. No changes were observed in the abundance or size of PSD-95 puncta at any of the tested concentrations, indicating that BHB alone has no effect at the synaptic level.

Interestingly, in the co-treatment experiments, we found that 1 mM and 2 mM of BHB effectively mitigated the adverse effects of PA on synaptic GluA1 and PSD95 levels, whereas 5 mM of BHB did not

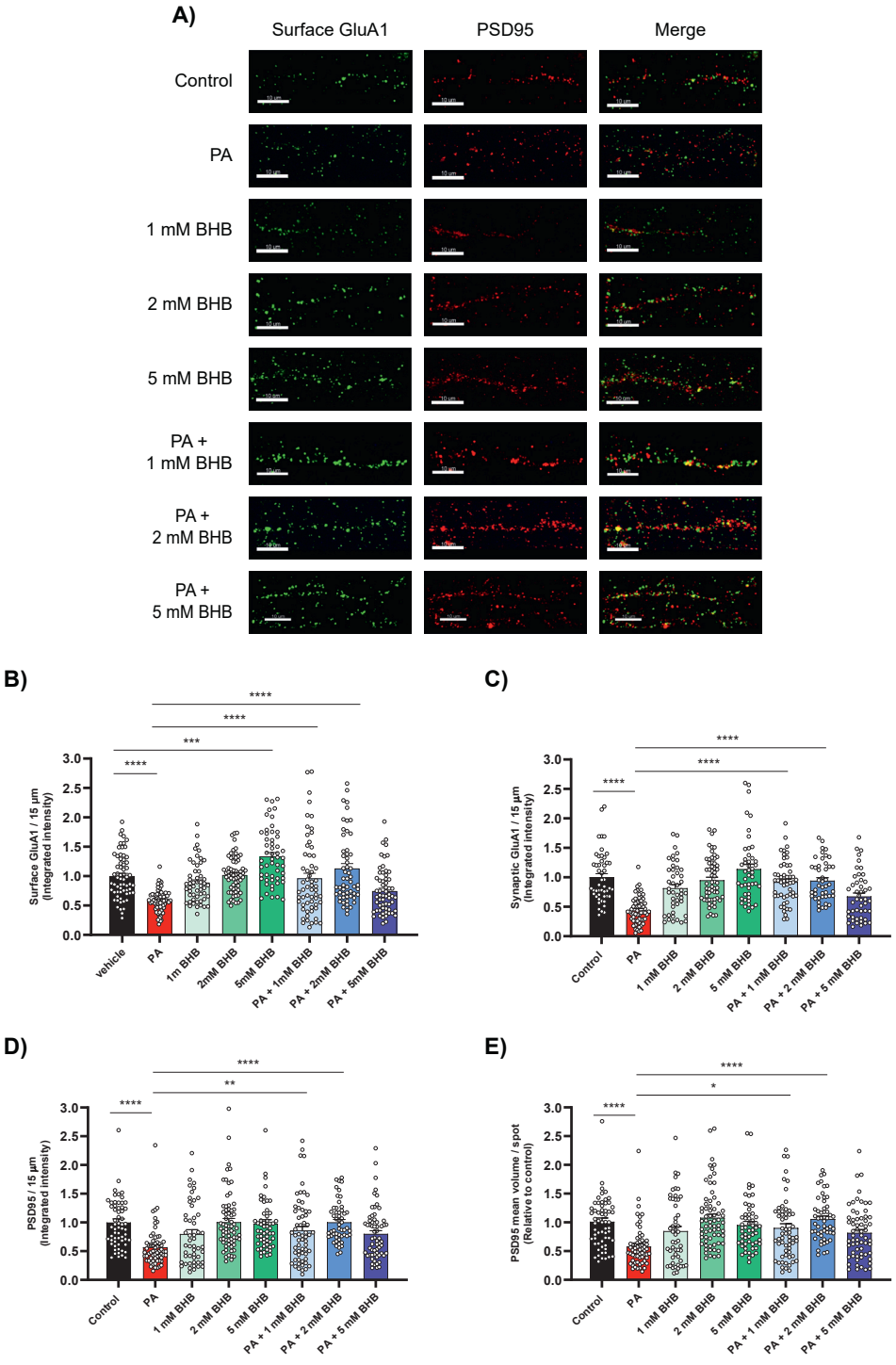

Figure 3: Short-term effects of PA and BHB on synaptic GluA1 levels in hippocampal neurons. Cultured neurons at 14 DIV were treated with PA (200 µM) and/or BHB (1, 2 or 5 mM). An equivalent amount of vehicle (BSA solution) was added to control neurons and BHB-treated ones to properly compare all the conditions. 2 h later, in non-permeabilized cells, GluA1 was detected by immunostaining. Then, cells were permeabilized, and a subsequent immunostaining was used to identify the synaptic marker PSD95. To determine synaptic GluA1 levels, the integrated intensity of GluA1 staining within the PSD95-defined ROI was quantified. Results in the graphs are normalized by the control and given as mean ± SEM from two independent experiments performed by biological duplicates. (A) Representative images of dendrites are shown (see Suppl. Fig. 4 for complete images). (B) Integrated intensity of surface GluA1 normalized by the control. Surface GluA1: Control ($n = 64$ neurons), PA ($n = 69$), 1 mM BHB ($n = 53$), 2 mM BHB ($n = 65$), 5 mM BHB ($n = 53$), PA + 1 mM BHB ($n = 60$), PA + 2 mM BHB ($n = 58$), and PA + 5 mM BHB ($n = 61$). (C) Normalized integrated intensity of synaptic GluA1. Synaptic GluA1: Control ($n = 49$), PA ($n = 58$), 1 mM BHB ($n = 45$), 2 mM BHB ($n = 59$), 5 mM BHB ($n = 46$), PA + 1 mM BHB ($n = 52$), PA + 2 mM BHB ($n = 45$), and PA + 5 mM BHB ($n = 47$). (D) Normalized integrated intensity of total PSD95. PSD95: Control ($n = 61$), PA ($n = 63$), 1 mM BHB ($n = 51$), 2 mM BHB ($n = 68$), 5 mM BHB ($n = 56$), PA + 1 mM BHB ($n = 61$), PA + 2 mM BHB ($n = 53$), and PA + 5 mM BHB ($n = 63$). (E) Mean volume of PSD95 spots normalized by the control. PSD95 volume: Control ($n = 61$), PA ($n = 63$), 1 mM BHB ($n = 51$), 2 mM BHB ($n = 68$), 5 mM BHB ($n = 56$), PA + 1 mM BHB ($n = 61$), PA + 2 mM BHB ($n = 53$), and PA + 5 mM BHB ($n = 63$). Scale bar of inset magnifications = 10 µm **, $P < 0.01$; ***, $P < 0.001$; and ****, $P < 0.0001$. One-way ANOVA followed by the Bonferroni test.

exhibit a significant beneficial impact (Figure 3C—E; blue bars). We think that excessively high concentrations of BHB likely have indirect counterproductive effects at the synapse level.

Since kinetic parameters in cortical mEPSC recordings suggested no changes in synaptic AMPAR subtype composition, we also analyzed GluA2 levels, given that GluA1-GluA2 heteromers are the dominant AMPARs at hippocampal synapses [40]. As expected, PA treatment led to a decrease in both surface and synaptic GluA2, an effect that was successfully prevented by co-administration of 2 mM BHB (Figure 4A—C).

Moreover, we confirmed that the PA negative effects were not attributable to reduced cell survival, as shown by the viability assay conducted 24 h post-treatment (Suppl. Figure 5A). Additionally, no significant alterations in neurite morphology were detected, as shown by the consistent MAP2 area percentage across all conditions following a 2-hour treatment (Suppl. Figure 5B). In line with the findings in cortical neurons, no changes were observed in total GluA1 levels, neither GluA2 nor PSD95 in hippocampal neurons treated with PA for 2 h, as demonstrated by Western blot (Suppl. Figure 5C). Additionally, the levels of GluA1 phosphorylated at serine 845 (pS845) —a post-translational modification traditionally associated with synaptic plasticity [41]— remained unchanged (Suppl. Figure 5C), consistent with previous observations [10].

Finally, we measured mEPSCs in primary hippocampal neurons following co-exposure to PA and BHB for 2 h (Figure 5A). The PA-induced reduction in AMPAR-mediated mEPSC amplitudes was reversed by co-administration of BHB (Figure 5B—C). As expected, BHB alone did not alter mEPSC amplitude in hippocampal neurons, consistent with observations made in cortical cultures (Suppl. Figure 5D). Cumulative amplitude histograms also revealed a distinct shift in the amplitude distribution toward smaller values under PA treatment in hippocampal neurons (Figure 5D), as observed in cortical ones. Furthermore, frequency and kinetic parameters (Figure 5E-G) confirmed the absence of alterations at the presynaptic level and in AMPAR subtype composition.

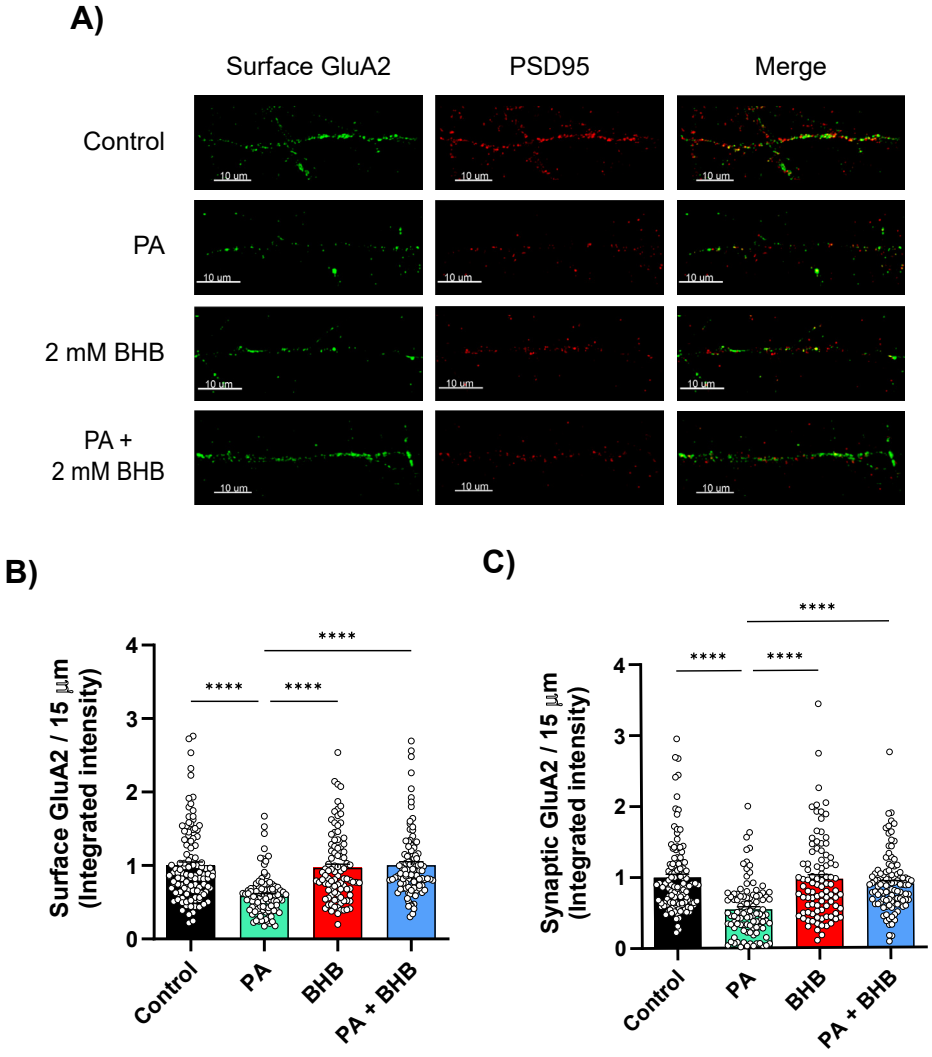

Figure 4: BHB prevents PA-mediated decrease in synaptic GluA2 levels in hippocampal neurons. Cultured neurons at 14DIV were treated with PA (200 μM) and/or BHB (2 mM) for 2 h. Surface and synaptic GluA2 levels were detected, analyzed, and quantified following the same approach as for GluA1 in the previous figure. Results in the graphs are normalized by the control and given as mean ± SEM from three independent experiments performed by biological duplicates. (A) Representative images of dendrites are shown. (B—C) The results in the graphs are the integrated intensity of surface (A) or synaptic (C) GluA2 normalized by the control given as the mean ± SEM. Surface GluA2: Control ($n = 116$ neurons), PA ($n = 101$), 2 mM BHB ($n = 94$), and PA + 2 mM BHB ($n = 103$). Synaptic GluA2: Control ($n = 120$), PA ($n = 100$), 2 mM BHB ($n = 94$), and PA + 2 mM BHB ($n = 104$). Scale bar of inset magnifications = 10 μm ****, $P < 0.0001$. One-way ANOVA followed by the Bonferroni test.

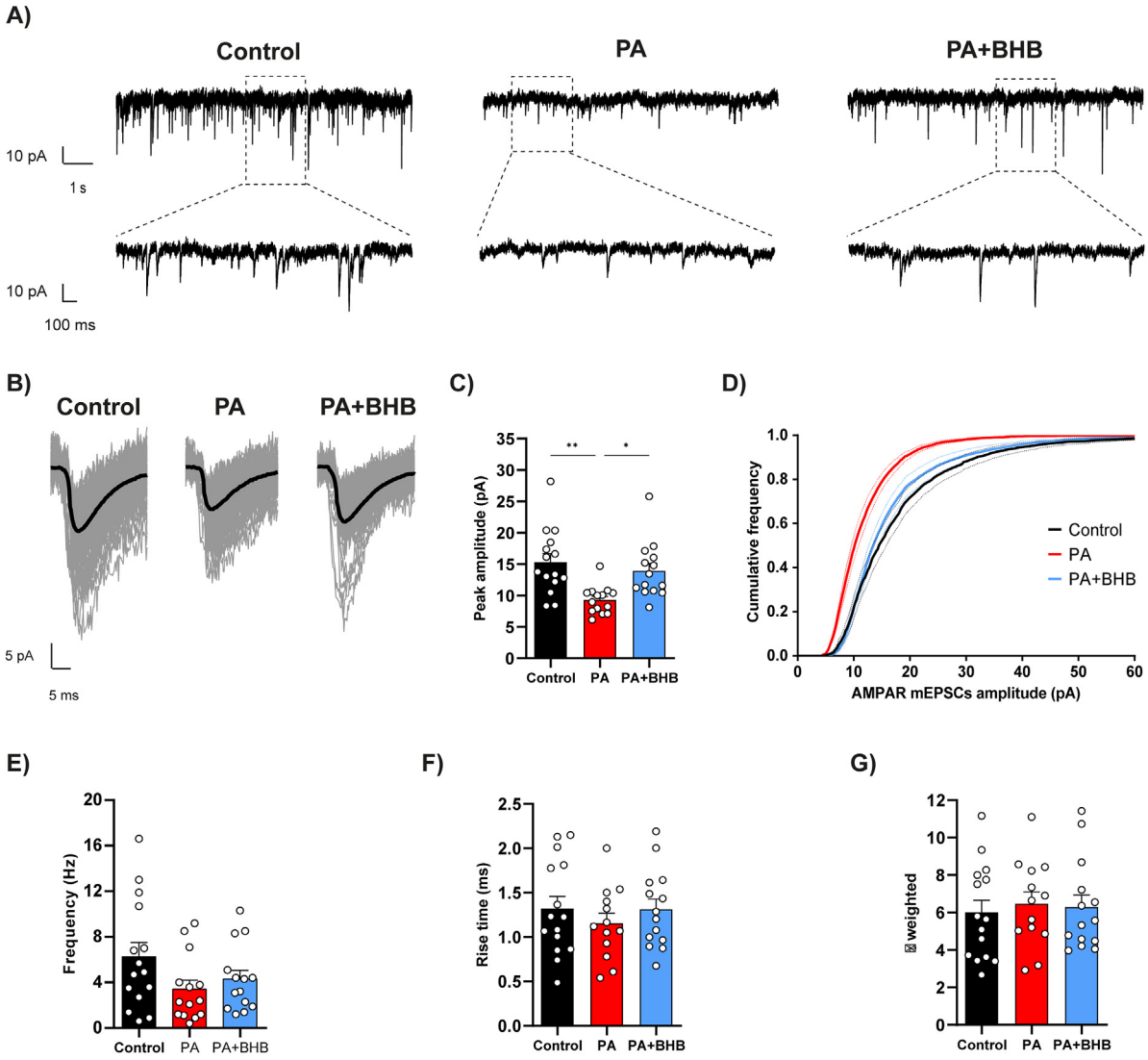

Figure 5: BHB counteracts PA-induced reduction of AMPAR-mediated mEPSCs amplitude in hippocampal neurons. Cultured neurons at 13–14 DIV were treated with PA (200 μM) or BHB (2 mM) for 2–3 h prior recordings. (A) Representative AMPAR-mediated mEPSCs. Membrane potential was held at −70 mV. (B) Examples of averaged mEPSCs (bold lines) from 3-, 3- and 5-minutes of time (control, PA, and PA + BHB, respectively) of the recordings shown in A. Control neurons exhibited a mean mEPSCs amplitude of −13.48 pA (average of 714 miniature events); PA-treated ones (central traces), −8.98 pA (297 events); and PA + BHB-treated ones, −11.71 pA (681 events). One hundred random individual mEPSCs events are shown in grey for each group. (C) AMPAR mEPSCs amplitude was decreased in PA-treated cells compared with control neurons (−15.34 ± 1.34 pA, $n = 15$; −9.29 ± 0.59 pA, $n = 14$; and −13.92 ± 1.19 pA, $n = 14$ for control, PA, and PA + BHB-treated neurons respectively). (D) Cumulative probability distribution of mEPSCs amplitude showing a leftward shift in amplitude for events of PA-treated neurons. Continuous lines represent the average for control (black line; $n = 15$ neurons), PA (red line; $n = 14$), and PA + BHB (blue line; $n = 14$). Thin lines denote the SEM. (E) AMPAR mEPSCs frequency was not altered with PA nor with PA + BHB (6,27 ± 1.24 Hz; 3.42 ± 0.77 Hz; and 4.29 ± 0.77 Hz; for control, PA, and PA + BHB, respectively). (F) AMPAR mEPSCs rise time was not altered with PA nor with PA + BHB (1.31 ± 0.14 ms; 1.16 ± 0.11 ms; and 1.31 ± 0.12 ms for control, PA, and PA + BHB, respectively). (G) AMPAR mEPSCs τ-weighted was not altered either with PA or with PA + BHB (6.00 ± 0.66 ms; 6.46 ± 0.64 ms; and 6.28 ± 0.65 ms; for control, PA, and PA + BHB, respectively). *, $P < 0.05$; and **, $P < 0.01$. One-way ANOVA followed by the Bonferroni test. (For interpretation of the references to color in this figure legend, the reader is referred to the Web version of this article.)

These findings suggest that the harmful effects of SFA on AMPAR synaptic abundance and synaptic transmission could be prevented by co-administration of BHB.

3.3. BHB restores palmitate-induced impairment in hippocampal synaptic plasticity

To explore whether the beneficial effects of BHB following PA treatment extend to evoked synaptic transmission and synaptic plasticity, we performed fEPSP recordings in the CA1 area of the hippocampus and whole-cell recordings from CA1 pyramidal cells in acute slices. Synaptic responses were elicited by stimulating Schaffer collateral (SC), and picrotoxin was included in the bath to block fast inhibitory synaptic transmission.

First, to test the effect of PA and BHB on basal synaptic transmission, I/O curves were conducted by increasing stimulation intensity (from 10 to 90 V) in hippocampal slices following short-term exposition (2 h) to PA (200 μM), BHB (2 mM), or a combination of both. Our results revealed a significant reduction in the slope of I/O curves under PA treatment compared with control slices, whereas BHB administration increased it (Figure 6A). Remarkably, PA and BHB co-administration demonstrated the ability of BHB to counteract the effects induced by PA.

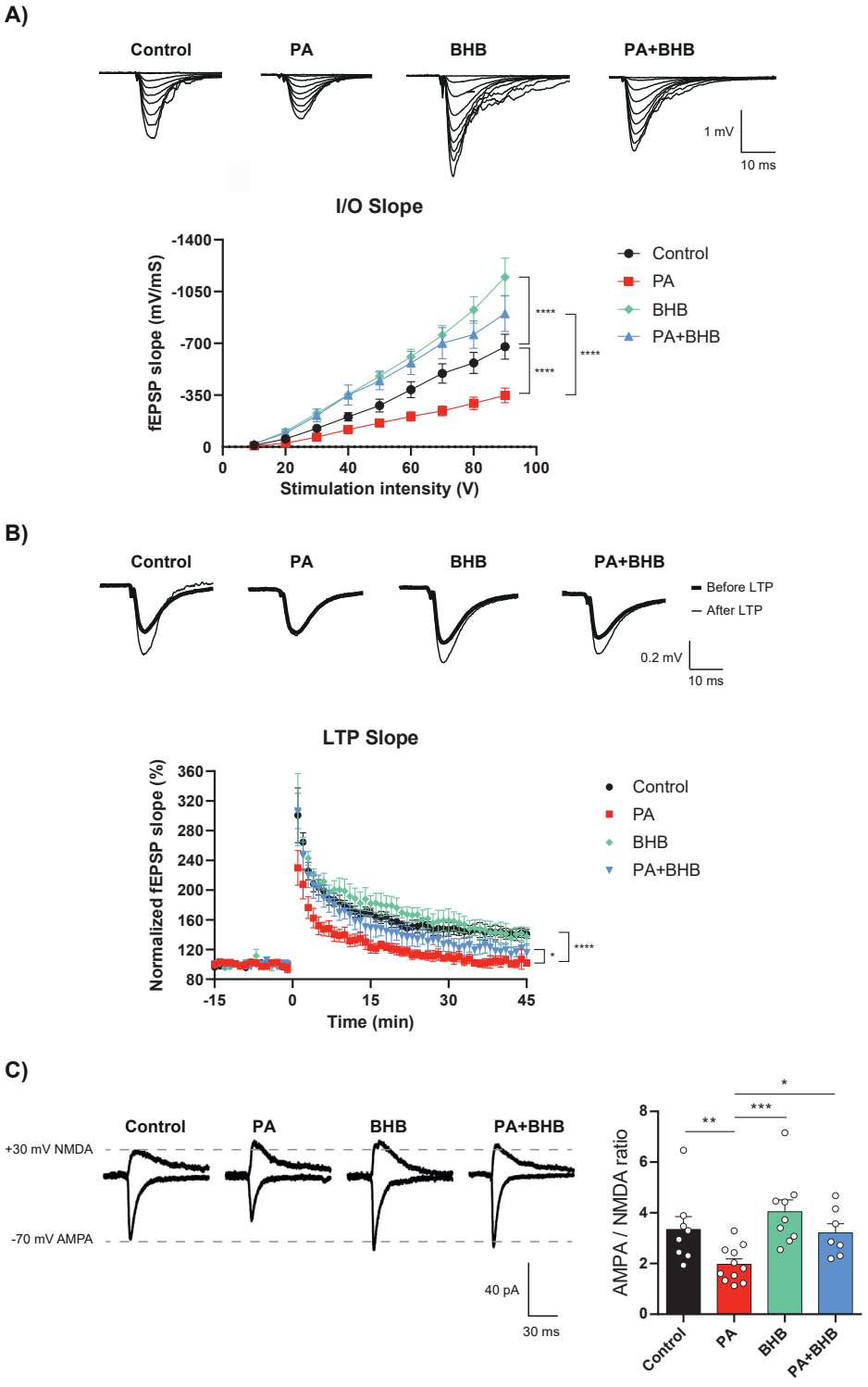

Figure 6: BHB ameliorates PA-induced changes in synaptic transmission and plasticity in hippocampal slices. (A) Representative fEPSPs evoked by stimulating the SC and summary graph showing the effect of PA, BHB and the combination of PA + BHB on I/O function. Results are expressed as mean ± SD. $n = 10–17$ slices/4 male mice per condition. Two-way ANOVA was followed by the Bonferroni test. (B) Representative fEPSPs and summary time−course plot of field recordings showing the effect of PA, BHB and the combination of PA + BHB on LTP magnitude. Data are expressed as the mean ± SD. $n = 3–4$ slices/3−4 male mice per condition. One-way ANOVA was followed by the Bonferroni. Representative traces of the baseline (thick lines) and the last 5 min of the time course after LTP induction (thin lines). (C) Representative traces of AMPA and NMDA receptor-mediated postsynaptic currents were recorded at −70 and + 30 mV, respectively. Summarizing bar graphs showing the effect of the different treatments on the AMPA/NMDA ratio. Data are represented as mean ± SEM. $n = 7–11$ cells/5−7 male mice per condition. Control (3.35 ± 0.50, $n = 8$), PA (1.97 ± 0.21, $n = 11$), BHB (4.05 ± 0.46, $n = 9$), and PA + BHB (3.21 ± 0.36, $n = 7$). One-way ANOVA followed by the Bonferroni test (A–B) or by the Sidakholm Test (C). *, $P < 0.05$; **, $P < 0.01$; ***$P < 0.001$; and ****, $P < 0.0001$.

We next analyzed the effect of PA and BHB on CA1 LTP. After a stable 15-minute baseline, LTP was induced by delivering high-frequency stimulation. Incubation with PA dampened LTP compared to control slices. On the other hand, BHB alone did not significantly affect the LTP magnitude (Figure 6B). However, it successfully prevented the LTP reduction induced by PA, when simultaneously administered. To test whether synaptic plasticity changes had a presynaptic origin, we measured the PPR, a metric linked to the probability of neurotransmitter release. PPR was unaffected across all analyzed conditions (Suppl. Figure 6A-C), indicating that the effects of PA and BHB are likely postsynaptic.

Finally, we calculated the AMPA/NMDA ratio by comparing the amplitudes of AMPAR and NMDAR-mediated EPSCs. PA significantly reduced the AMPA/NMDA ratio, an effect that was prevented by co-treatment with BHB (Figure 6C). These results suggest that the effect of PA on synaptic transmission is likely due to a reduction in AMPARs but not in NMDARs-mediated transmission.

In summary, SFA and ketone bodies affected postsynaptic but not presynaptic function. In addition, BHB restored the PA-mediated impairment in synaptic transmission and plasticity. Consistent with our observations in cultured neurons, our findings in hippocampal slices further support the idea that PA and BHB exert their effects, at least in part, by regulating AMPARs.

3.4. BHB counteracts the cognitive impairment mediated by a saturated fatty acid-rich diet in mice

To assess whether the beneficial effects of BHB extend to mitigating PA-induced cognitive impairment, we conducted *in vivo* experiments in mice. Specifically, we explored whether daily administration of BHB could counteract the adverse effects of an SFAD on memory task performance. To achieve this goal, 5-week-old mice were fed SFAD (constituting 34.8% of calories from SFA) or a CD (10% of calories from fat) for seven weeks. Previous studies using mice of similar age and diet duration, as well as comparable SFA content, have shown increased hippocampal levels of palmitic acid [10]. Additionally, our group previously demonstrated that male mice on a SFAD exhibit increased plasma leptin levels, hypertrophy of white adipose tissue, and hepatic fat accumulation [42,43].

Based on finding from [44], we decided to perform an intragastric administration of 100 mg/kg/day BHB in mice or an equal volume of vehicle (water) throughout this period. Acutely, this dosage effectively increased BHB levels in both plasma and the brain, with levels reaching a maximum within 30 min post-administration in plasma and within 4 h in the brain (Suppl. Figure 7A-B). Body weight and food intake were monitored weekly over the course of the experiment. Finally, behavioral tests were conducted, and the animals were euthanized to obtain cortical and hippocampal brain tissues for BHB level analysis and protein detection by WB, respectively.

Results show that chronic BHB administration effectively increased plasma and brain BHB levels compared to those receiving the vehicle, especially in the SFAD-fed mice (Figure 7A—B). However, the SFAD *per se* failed to raise plasma and brain BHB levels compared to the CD, which reflects the lack of ketosis, as the carbohydrate content in this diet was moderate (31%) [45].

We also analyzed GluA1, GluA2, and PSD95 protein levels in hippocampal extracts from these animals. As expected, no significant differences were found between groups (Suppl. Figure 8), suggesting that these measurements represent total protein levels rather than synaptic localization. Notably, mice fed the SFAD showed a reduction in phosphorylated GluA1 at serine 845 (pS845-GluA1), the modification typically linked to synaptic GluA1 localization [41]. In contrast, no significant changes were observed in mice treated with BHB. However, these results should be interpreted with caution, as pS845-GluA1 constitutes only a small fraction of total synaptic GluA1 [46,47].

Regarding body weight and food intake (Figure 7C—F), male exposed to the SFAD revealed a tendency toward higher body weight, with statistical significance only observed between weeks 5—7 (Figure 7C). Moreover, SFAD-fed male also tended to consume more kilocalories (Figure 7E), which may help explain the observed weight gain. These effects were absent in females (Figure 7D,F), which aligns with the well-documented hormone-dependent resistance of adult females to diet-induced obesity compared to males [12]. Notably, SFAD-fed male mice supplemented with BHB did not display this trend of weight gain and showed a tendency toward reduced food intake. Results suggest that BHB prevents body weight gain triggered by SFAD in male mice. As expected, hepatic triglyceride levels were increased in SFAD-fed males compared to CD group, whereas this increase was not significant in females (Suppl. Figure 9A-B). Interestingly, in BHB-supplemented SFAD-fed males, the elevation in hepatic triglyceride content was attenuated. In contrast, hepatic cholesterol levels were not significantly elevated in SFAD-fed animals compared to CD group, and BHB administration had no substantial effect on this parameter (Suppl. Figure 9C-D). Although our primary objective was to investigate the cognitive effects of BHB rather than its impact on metabolism, food intake, or hepatic fat accumulation, the results indicate that its potential metabolic benefits warrant further investigation, with an emphasis on potential sex-specific responses.

To examine the cognitive performance of mice, two behavioral tests were conducted at the end of the experiment: NORT and OLT. NORT included short-term memory (2 h post-habituation) and long-term memory (24 h later), both assessed using the DI, a metric reflecting the animal's ability to recognize and remember a previously encountered object. While no significant differences were observed among CD-fed groups, mice exposed to SFAD exhibited substantial cognitive impairments completely prevented by concurrent BHB administration at both short and long-term memory tests (Figure 8A—B). Interestingly, all groups —except those fed SFAD alone— showed a clear preference for the novel object (Suppl. Figure 10A-B), further supporting the protective effect of BHB on memory function.

In the assessment of spatial learning evaluated through OLT, a remarkable difference was also found between CD and SFAD (Figure 8C), corroborating the detrimental effects of SFA on brain functions. Once more, BHB co-administration demonstrated its efficacy in counteracting the harmful effects of an SFAD, as evidenced by the animals' preference for exploring the object in the new location (Suppl. Figure 10C). In this context, the examination of locomotor activity revealed that, when administered with SFAD, BHB increased the distance traveled by mice compared to the other experimental groups (Figure 8D), suggesting heightened locomotor activity and energy. By contrast, no differences were found in the time spent in the center or periphery, nor in the number of rearings and grooming across all the groups (Suppl. Figure 10D-G), indicating that SFAD feeding and BHB administration unaffected exploratory and anxiety-like behaviors. Furthermore, the absence of overall changes in food intake (Figure 7E—F), along with normal observations of deposits and urination (Suppl. Figure 10H-I), suggested that gastrointestinal distress associated with BHB ingestion can be excluded, an issue previously reported with higher doses of ketone salts in some humans [48].

Collectively, our findings reveal the beneficial role of BHB supplementation in counteracting the detrimental effects of a high-saturated-fat diet on learning and memory abilities in mice. These *in vivo* results are in line with our *in vitro* observations, confirming that BHB alone

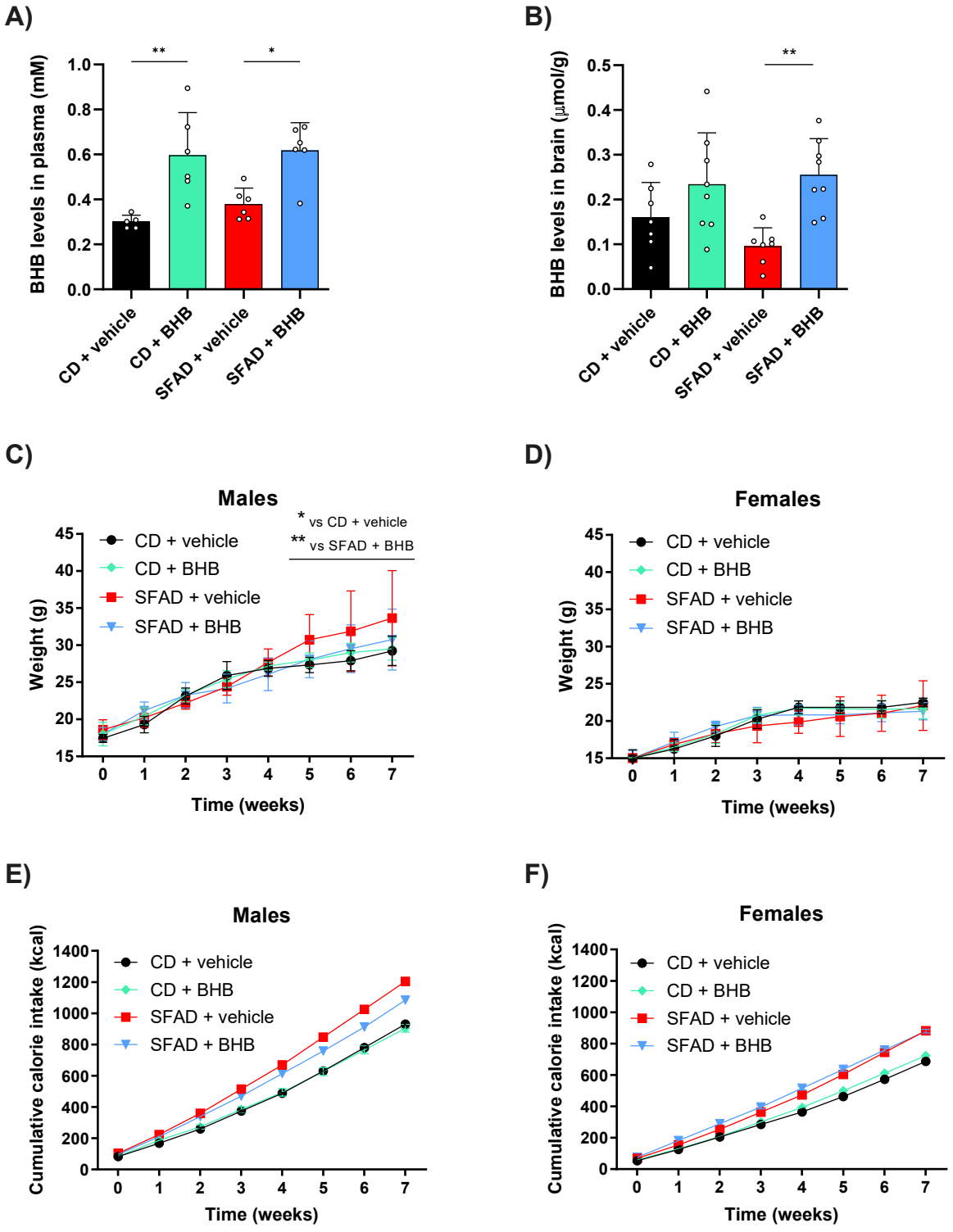

Figure 7: Effect of BHB administration on body weight gain mediated by SFAD. 5-weeks old-mice were divided into 4 groups: CD (10% of kcal from FA) + vehicle (equal amount of water), $n = 4♀+7♂$; CD + BHB administration (100 mg/kg/day), $n = 4♀+5♂$; SFAD (49% of kcal from SFA) + vehicle, $n = 6♀+5♂$; and SFAD + BHB, $n = 5♀+6♂$. Animals were maintained for 7 weeks under these feeding conditions and submitted to behavior test 3 days before the sacrifice to obtain blood and tissue samples. (A) The BHB levels in plasma 30-min post BHB administration. To achieve this, an additional smaller cohort was fed for 7 weeks, administrated daily, and sacrificed at 30-min post BHB administration. The results in the graphs are the mean ± SD. CD + vehicle (0.30 ± 0.03, $n = 5$), CD + BHB (0.60 ± 0.19, $n = 6$), SFAD + vehicle (0.38 ± 0.07, $n = 6$), and SFAD + BHB (0.62 ± 0.12, $n = 6$). (B) The BHB levels in brain 2-hours post BHB administration. The results in the graphs are the mean ± SD. CD + vehicle (0.16 ± 0.08, $n = 7$), CD + BHB (0.23 ± 0.12, $n = 8$), SFAD + vehicle (0.10 ± 0.04, $n = 7$), and SFAD + BHB (0.26 ± 0.08, $n = 8$). (C–D) The animals were weighed weekly. Male and female weight is shown in C and D, respectively. Data are represented as mean ± SD from $n = 5–7$/group. (E–F) Cumulative food intake stratified by sex is shown in kcal. Data are represented as mean ± SD, obtained from $n = 4–6$/group. For animal welfare reasons, mice were group-housed (2–6 per cage) as indicated. Males: CD + vehicle ($n = 2$ cages, 4 and 3 mice in each cage), CD + BHB ($n = 2$, 2 and 3 mice in each cage), SFAD + vehicle ($n = 1$; 5 mice), and SFAD + BHB ($n = 1$, 6 mice). Females: CD + vehicle ($n = 1$, 4 mice), CD + BHB ($n = 1$, 4 mice), SFAD + vehicle ($n = 1$; 6 mice), and SFAD + BHB ($n = 2$, 2 and 3 mice in each cage). *, $P < 0.05$; and **, $P < 0.01$. One-way ANOVA was followed by the Bonferroni.

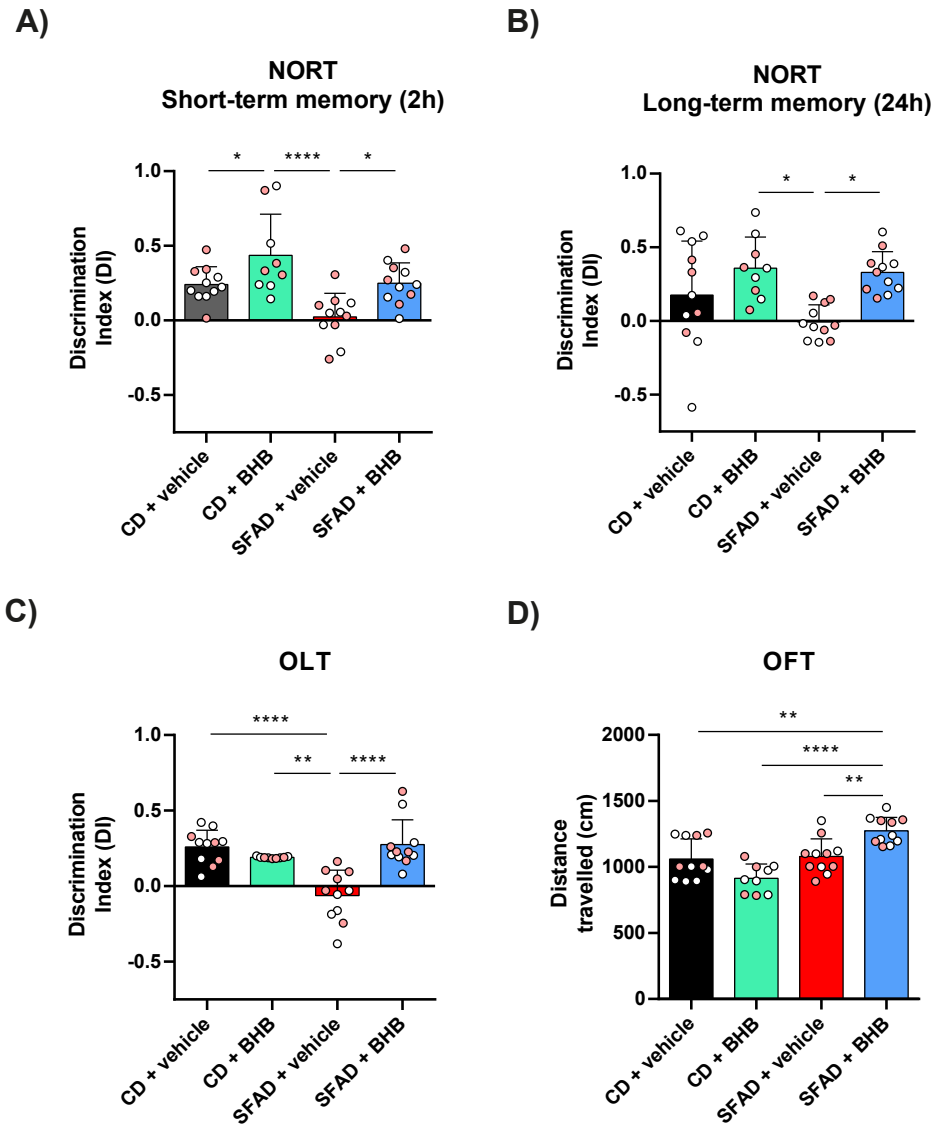

Figure 8: Effect of BHB administration in cognitive impairment mediated by SFAD. (A–C) NORT was performed 2 h (A) and 24 h (B) after the habituation phase, respectively, to assess recognition memory. OLT was performed to evaluate spatial memory (C). The results of the DI in the graphs are the mean ± SD. NORT 2 h: CD + vehicle (0.24 ± 0.12, $n = 11$), CD + BHB (0.44 ± 0.28, $n = 9$), SFAD + vehicle (0.02 ± 0.16, $n = 11$), and SFAD + BHB (0.25 ± 0.14, $n = 11$). NORT 24 h: CD + vehicle (0.18 ± 0.37, $n = 11$), CD + BHB (0.36 ± 0.21, $n = 9$), SFAD + vehicle (−0.01 ± 0.12, $n = 11$), and SFAD + BHB (0.33 ± 0.14, $n = 11$). OLT: CD + vehicle (0.26 ± 0.03, $n = 11$), CD + BHB (0.19 ± 0.002, $n = 9$), SFAD + vehicle (−0.06 ± 0.05, $n = 11$), and SFAD + BHB (0.26 ± 0.05, $n = 11$). (D) Locomotor activity was measured using OFT. Data are represented as mean ± SD. Locomotor activity: CD + vehicle (1059 ± 154, $n = 11$), CD + BHB (914 ± 109, $n = 9$), SFAD + vehicle (1079 ± 134, $n = 11$), and SFAD + BHB (1274 ± 101, $n = 11$). Values from males are represented by white spots, while values from females are shown as pink spots. *, $P < 0.05$; **, $P < 0.01$; and ****, $P < 0.0001$. One-way ANOVA followed by Bonferroni test. (For interpretation of the references to color in this figure legend, the reader is referred to the Web version of this article.)

does not influence cognitive function, but can reverse the harmful cognitive effects induced by saturated fats.

4. DISCUSSION

There is a noteworthy surge in the popularity of high-fat, low-carbohydrate diets for body weight management and for obesity and diabetes treatment [49–51]. In addition, these diets have been proposed as promising strategies to prevent cognitive decline [15]. However, their widespread application is limited by associated adverse effects [16,17]. In the present study, we demonstrate that intragastric administration of BHB successfully counteracts the memory and learning impairments induced by SFAD in mice. We attribute these effects to the ability of BHB to prevent PA-induced synaptic alterations.

4.1. BHB restores GluA1 synaptic levels and plasticity decreased by palmitate

Alterations in the expression of GluA1 or deregulations of its trafficking towards the PM are linked to impaired synaptic plasticity and cognition [6,7]. Our study reveals that PA treatment significantly decreases surface GluA1 levels, whereas OA, DHA, and BHB increase them in hippocampal and cortical cultured neurons. Our findings align with existing literature showing the beneficial effects of unsaturated and the negative effects of saturated fatty acids on synaptic plasticity and cognition [12,14,52–54].

Regarding PA, previous studies showed its ability to reduce AMPA sensitivity in cortical neurons, with no observable changes on NMDA sensitivity [14], suggesting a specific effect of PA on AMPARs, in accordance with our results. Other studies have examined the impact of PA in combination with insulin, revealing that the co-treatment caused GluA1 dephosphorylation at S845 and hyper-palmitoylation, concurrently downregulating its recruitment to the PM, and inhibiting AMPAR currents and their potentiation [10]. Our study demonstrates that PA *per se* is sufficient to reduce both surface and synaptic levels of GluA1 and GluA2, resulting in a decrease in AMPARs-mediated currents and synaptic plasticity. However, we did not observe a significant reduction in GluA1 phosphorylation at S845 with PA treatment alone. Notably, previous studies analyzing the stoichiometry of phosphorylated AMPARs have shown that less than 0.1% of GluA1 is phosphorylated at S845 [47], suggesting that most synapses likely contain no phosphorylated AMPAR. Therefore, even in the absence of changes in pS845 levels, the analysis of surface and synaptic GluA1 levels correlates closely with synaptic transmission and plasticity, with PA exerting a deleterious effect on these processes.

By contrast, the influence of BHB supplementation on surface or synaptic GluA1 and GluA2 levels has not been previously evaluated. Here, we demonstrate that BHB treatment, even with short exposures, can counteract the negative effects of PA on GluA1 and GluA2 surface and synaptic levels, AMPAR-mediated currents, and synaptic plasticity. It is important to notice that BHB alone has no effects on AMPAR synaptic abundance or plasticity. However, high doses of BHB increase surface GluA1 levels. These results suggest that the BHB-mediated increase in surface GluA1 might be confined to the perisynaptic zone—a subset of GluA1-containing AMPARs that could be swiftly and transiently mobilized to synapses under specific conditions, being involved in the reversibility of both synaptic and dendritic spine modifications [55,56].

Furthermore, PA and BHB effects on synaptic transmission and plasticity are mainly postsynaptic, as supported by the lack of alterations in the PPR and mEPSC frequency. Moreover, the reduction in the AMPA/NMDA ratio observed in response to PA indicates that NMDARs are likely not involved in PA-triggered synaptic changes, as previously reported [10,57]. Moreover, mEPSC data points to an unchanged subtype composition, suggesting that the trafficking of all AMPAR subunits is affected similarly by PA treatment. Interestingly, a high-fat diet induces both GluA1 and GluA2 palmitoylation [10], a post-translational modification that decreases the surface abundance of both subunits [58], according to our results.

Noteworthy, other studies obtained similar results in a different context. BHB treatment effectively prevented the impairment of LTP mediated by several injuries in hippocampal slices (such as exposure to excitotoxic levels of NMDA, rotenone toxin, or hydrogen peroxides), without inducing any alterations when administrated alone [35—37]. Furthermore, in a mouse model of Alzheimer's disease, BHB-mediated improvements in cognition were associated with increased LTP, whereas in young or healthy animals, a ketogenic diet unaffected LTP [59,60]. These data suggest that BHB is effective in restoring synaptic structure and function when previously impaired by harmful agents or conditions, but it does not enhance synaptic efficiency under normal or healthy physiological states.

4.2. BHB supplementation counteracts the cognitive impairment triggered by SFAD

Exposure to obesogenic dietary components, such as SFA, contributes to cognitive decline compared to isocaloric standard diets at any life stage [12]. As expected, in our study, the consumption of SFAD (49% kcal from fat and 31% from carbohydrates) in mice induced memory and learning impairments equally in both sexes, although weight gain and hepatic triglyceride content was increased in males but not in female mice. This underscores that the cognitive negative impact may precede or surpass the adverse metabolic effects of SFAD. Similar results were obtained with a short-term administration of a high-fat, high-sucrose diet, which caused cognitive impairment in the absence of overt metabolic disturbances [61]. Remarkably, even a single week of high-fat diet was sufficient to induce memory deficits, despite no detectable changes in body weight [62].

Despite the great popularity of the ketogenic diet as a strategy for managing body weight, evidence demonstrates that it is equally effective for weight loss as diets with higher carbohydrate content [63]. The consumption of ketone esters as supplements (often BHB linked to an ester molecule) has been associated with satiety and increased energy expenditure, particularly in the context of high-carbohydrate diets, contributing to an enhancement in weight loss. Similarly, in our study, the administration of BHB resulted in reduced body weight in male mice with an SFAD, possibly due to increased energy expenditure and reduced food intake, as suggested by heightened locomotor activity and a trend toward lower caloric consumption. Notably, increased locomotor activity following BHB administration has also been reported in animal models of neurodegeneration, whereas no such effects were observed in healthy controls [21,64,65]. This aligns with our findings, in which BHB administration did not alter locomotor activity in CD-fed mice, suggesting that the beneficial effects of BHB may emerge under conditions of neurological dysfunction or metabolic stress.

BHB *per se* under a standard diet affects short-term memory but cannot induce a sustained enhancement in spatial learning and long-term memory. These results align perfectly with a previous report where BHB supplementation improved short-term memory but not long-term in healthy animals [59]. Interestingly, we took a significant step beyond previous publications by demonstrating that BHB administration successfully prevented SFAD's harmful effect on cognition. The oral administration of a single daily dose of BHB was sufficient to neutralize the adverse effects of a high-fat diet on both short- and long-term memory, as well as exploratory interest, in adult mice. BHB administration did not lead to an increase in pS845 GluA1 levels in SFAD-fed animals, consistent with observations in treated cortical and hippocampal neuronal cultures. Therefore, even in the absence of changes in pS845 GluA1 levels, the preservation of synaptic AMPARs and associated improvements in neuroplasticity may underline the cognitive protective effects of BHB under SFAD exposure. Our findings point out that the cognitive benefits observed with ketogenic diets may be (at least partially) mediated by the ketone bodies produced during their implementation, which counteract the harmful effects of the SFA present in the diet. Notably, although human studies remain inconclusive, ketogenic-based formulas used as dietary supplements appear to more consistently enhance learning and memory performance than ketogenic diets themselves, especially in older populations and patients with Alzheimer's disease [12]. Furthermore, our results provide a potential explanation for the cognitive benefits induced by intermittent fasting [66]. During fasting, the hypoglycemia response triggers the release of SFA from adipose tissue into the bloodstream, whereas the liver produces ketone bodies. In such situations, we propose that the elevated levels of circulating ketone bodies not only serve as the primary energy source for neurons but also mitigate the negative impact of endogenous SFA on synaptic function and cognition. Considering that a ketogenic diet and intermittent fasting often face challenges in lasting adherence [67], dietary BHB supplementation may yield more satisfactory long-term outcomes

to prevent weight gain and cognitive impairments linked to metabolic diseases.

It is important to note that the ketogenic diet has been utilized for a century as a protective strategy in epileptic patients [68]. However, this has been attributed to the medium-chain triglyceride decanoic acid, which is often elevated in this type of diet and blocks seizures through the direct inhibition of AMPARs, rather than ketone bodies themselves [69]. Clinically relevant concentration of BHB *per se* does not directly alter excitatory synaptic transmission [70,71] an effect that perfectly aligns with our findings on synaptic AMPARs and mEPSCs in cultured neurons. Although the L-(+)-BHB isomer has been shown to exert anticonvulsant effects *in vivo* —effects not observed with the D-(+)-isomer— these outcomes may be attributed to dibenzylamine, a contaminant found in commercial L-BHB formulations [71,72]. Importantly, these authors demonstrated that neither isomer affected AMPARs-mediated currents, which aligns with our findings using the D/L-BHB racemic mixture.

The molecular mechanisms by which ketone bodies induce synaptic and cognitive changes appear diverse. It has been reported that β-hydroxybutyrate (BHB) increases brain-derived neurotrophic factor (BDNF) levels and promotes regeneration [23], whereas also reducing inflammation and oxidative stress [19–22]. Additionally, BHB has been shown to β-hydroxybutyrylate proteins, thereby altering their function [25]. It can also induce epigenetic modifications and chromatin remodeling [73–76]. These findings suggest that the changes caused by such diets or supplements may have long-term effects, potentially even across generations. Further research is required to gain a deeper understanding of the modifications and molecular pathways activated by KBs supplementation in the brain.

In summary, our findings demonstrate that BHB effectively mitigates the adverse effects of PA on synaptic GluA1 abundance and plasticity. Additionally, BHB administration in mice successfully prevents the cognitive decline associated with a saturated high-fat, moderate-carbohydrate diet, which closely resembles the Western diet commonly consumed worldwide (characterized by a high intake of animal-based foods, fats, and simple sugars). Therefore, BHB supplementation could be a promising nutritional strategy to counteract the negative impacts of a Western diet on cognitive function.

DECLARATION OF GENERATIVE AI IN SCIENTIFIC WRITING

AI-assisted technologies have been exclusively used in the writing process to enhance the manuscript's readability and language.

CRediT AUTHORSHIP CONTRIBUTION STATEMENT

Rocío Rojas: Investigation, Formal analysis, Data curation. **Christian Griñán-Ferré:** Investigation, Funding acquisition, Formal analysis. **Aida Castellanos:** Investigation, Formal analysis, Data curation. **Ernesto Griego:** Writing – review & editing, Investigation. **Marc Martínez:** Investigation. **Juan de Dios Navarro-López:** Funding acquisition. **Lydia Jiménez-Díaz:** Funding acquisition. **José Rodríguez-Álvarez:** Funding acquisition. **David Soto del Cerro:** Investigation, Funding acquisition, Formal analysis. **Pablo E. Castillo:** Writing – review & editing, Supervision, Funding acquisition. **Mercè Pallàs:** Funding acquisition, Conceptualization. **Núria Casals:** Writing – review & editing, Supervision, Project administration, Funding acquisition, Conceptualization. **Rut Fadó:** Writing – original draft, Supervision, Investigation, Formal analysis, Data curation, Conceptualization.

DECLARATION OF COMPETING INTEREST

The authors declare that they have no competing interests.

FUNDING SOURCES

This work was supported by the Spanish Ministry of Science and Innovation (MCIN) (PID2020-114953RB-C22 to N.C.; PID2022-139016OA-I00 and PDC2022-133441-I00 to C.G-F. and M.P.; PID2020-117510RB-I00 to J.R.A.; PID2020-119932 GB-I00 and María de Maeztu Unit of Excellence CEX2021-001159-M to M.P. and D.S.), the CIBEROBN (CB06/03/0001 to N.C.), the FEDER Regional European Development Fund and CIBERNED (CB06/05/0042 to J.R.A.), the Generalitat de Catalunya (2021 SGR 00357 to C.G-F. and M.P.), and the NIH grants (R01MH116673, R01MH125772, and R01NS113600 to P.E.C. and E.G.).

DATA AVAILABILITY

Data will be made available on request.

APPENDIX A. SUPPLEMENTARY DATA

Supplementary data to this article can be found online at https://doi.org/10.1016/j.molmet.2025.102207.

REFERENCES

[1] World Health Organization. Dementia: number of people affected to triple in next 30 years. http://www.who.int/fr/news-room/detail/07-12-2017-dementia-number-of-people-affected-to-triple-in-next-30-years. [Accessed 7 December 2017].

[2] Dye L, Boyle NB, Champ C, Lawton C. The relationship between obesity and cognitive health and decline. Proc Nutr Soc 2017;76(4):443–54. https://doi.org/10.1017/S0029665117002014.

[3] Golomb BA, Bui AK. A fat to forget: trans fat consumption and memory. PLoS One Jun. 2015;10(6). https://doi.org/10.1371/JOURNAL.PONE.0128129.

[4] Okereke OI, Rosner BA, Kim DH, Kang JH, Cook NR, Manson JE, et al. Dietary fat types and 4-year cognitive change in community-dwelling older women. Ann Neurol Jul 2012;72(1):124–34. https://doi.org/10.1002/ANA.23593.

[5] Baym CL, Khan NA, Monti JM, Raine LB, Drollette ES, Moore RD, et al. Dietary lipids are differentially associated with hippocampal-dependent relational memory in prepubescent children. Am J Clin Nutr May 2014;99(5):1026–33. https://doi.org/10.3945/AJCN.113.079624.

[6] Hanley JG. Subunit-specific trafficking mechanisms regulating the synaptic expression of Ca2+-permeable AMPA receptors. Semin Cell Dev Biol 2014;27:14–22. https://doi.org/10.1016/j.semcdb.2013.12.002.

[7] Jurado S. AMPA receptor trafficking in natural and pathological aging. Front Mol Neurosci Jan. 2018;10. https://doi.org/10.3389/FNMOL.2017.00446.

[8] Khazen T, Hatoum OA, Ferreira G, Maroun M. Acute exposure to a high-fat diet in juvenile male rats disrupts hippocampal-dependent memory and plasticity through glucocorticoids. Sci Rep 2019;9(1):1–10. https://doi.org/10.1038/s41598-019-48800-2.

[9] Beilharz JE, Maniam J, Morris MJ. Short exposure to a diet rich in both fat and sugar or sugar alone impairs place, but not object recognition memory in rats. Brain Behav Immun 2014;37:134–41. https://doi.org/10.1016/j.bbi.2013.11.016.

[10] Spinelli M, Fusco S, Mainardi M, Scala F, Natale F, Lapenta R. Brain insulin resistance impairs hippocampal synaptic plasticity and memory by increasing

GluA1 palmitoylation through. Nat Commun 2017;8(1):1—14. https://doi.org/10.1038/s41467-017-02221-9.

[11] Granholm AC, Bimonte-Nelson HA, Moore AB, Nelson ME, Freeman LR, Sambamurti K. Effects of a saturated fat and high cholesterol diet on memory and hippocampal morphology in the middle-aged rat. J Alzheim Dis 2008;14(2):133—45. https://doi.org/10.3233/JAD-2008-14202.

[12] Fadó R, Molins A, Rojas R, Casals N. Feeding the brain: effect of nutrients on cognition, synaptic function, and AMPA receptors. Nutrients Oct. 2022;14(19). https://doi.org/10.3390/NU14194137.

[13] McLean FH, Campbell FM, Sergi D, Grant C, Morris AC, Hay EA, et al. Early and reversible changes to the hippocampal proteome in mice on a high-fat diet. Nutr Metab 2019;16(1):1—12. https://doi.org/10.1186/s12986-019-0387-y.

[14] Loehfelm A, Elder MK, Boucsein A, Jones PP, Williams JM, Tups A. Docosahexaenoic acid prevents palmitate-induced insulin-dependent impairments of neuronal health. FASEB (Fed Am Soc Exp Biol) J 2020;34(3):4635—52. https://doi.org/10.1096/fj.201902517R.

[15] Vinciguerra F, Graziano M, Hagnäs M, Frittitta L, Tumminia A. Influence of the mediterranean and ketogenic diets on cognitive status and decline: a narrative review. Nutrients Apr. 2020;12(4). https://doi.org/10.3390/nu12041019.

[16] Patikorn C, Campbell FM, Sergi D, Grant C, Morris AC, Hay EA, et al. Effects of ketogenic diet on health outcomes: an umbrella review of meta-analyses of randomized clinical trials. BMC Med Dec 2023;21(1). https://doi.org/10.1186/S12916-023-02874-Y.

[17] Crosby L, Saidoung P, Pham T, Phisalprapa P, Lee YY, Varady KA, et al. Ketogenic diets and chronic disease: weighing the benefits against the risks. Front Nutr Jul. 2021;8. https://doi.org/10.3389/FNUT.2021.702802.

[18] Volek JS, Kackley ML, Buga A. Nutritional considerations during major weight loss therapy: focus on optimal protein and a low-carbohydrate dietary pattern. Curr Nutr Rep Sep. 2024;13(3):422—43. https://doi.org/10.1007/S13668-024-00548-6.

[19] Shimazu T, Hirschey MD, Newman J, He W, Shirakawa K, Le Moan N, et al. Suppression of oxidative stress by β-hydroxybutyrate, an endogenous histone deacetylase inhibitor. Science Jan 2013;339(6116):211—4. https://doi.org/10.1126/SCIENCE.1227166.

[20] Shippy DC, Wilhelm C, Viharkumar PA, Raife TJ, Ulland TK. β-Hydroxybutyrate inhibits inflammasome activation to attenuate Alzheimer's disease pathology. J Neuroinflammation Sep. 2020;17(1). https://doi.org/10.1186/s12974-020-01948-5.

[21] Yamanashi T, Iwata M, Shibushita M, Tsunetomi K, Nagata M, Kajitani N, et al. Beta-hydroxybutyrate, an endogenous NLRP3 inflammasome inhibitor, attenuates anxiety-related behavior in a rodent post-traumatic stress disorder model. Sci Rep Dec 2020;10(1). https://doi.org/10.1038/S41598-020-78410-2.

[22] Yang X, Wang R, Zhou H, Wang L, Wang R, Li H, et al. β-hydroxybutyrate alleviates learning and memory impairment through the SIRT1 pathway in D-Galactose-Injured mice. Front Pharmacol 2021;12(Nov). https://doi.org/10.3389/FPHAR.2021.751028.

[23] Ari C, D'Agostino DP, Cha BJ. Neuroregeneration improved by Sodium-D,L-Beta-Hydroxybutyrate in primary neuronal cultures. Pharmaceuticals Aug. 2024;17(9):1160. https://doi.org/10.3390/PH17091160.

[24] Hersant H, Grossberg G. The ketogenic diet and alzheimer's disease. J Nutr Health Aging Jun. 2022;26(6):606—14. https://doi.org/10.1007/S12603-022-1807-7.

[25] Han W, Zhang B, Zhao W, Zhao W, He J, Qiu X, et al. Ketogenic β-hydroxybutyrate regulates β-hydroxybutyrylation of TCA cycle-associated enzymes and attenuates disease-associated pathologies in Alzheimer's mice. Aging Cell Jan 2025;24(1). https://doi.org/10.1111/ACEL.14368.

[26] Wu Y, Gong Y, Luan Y, Li Y, Liu J, Yue Z, et al. BHBA treatment improves cognitive function by targeting pleiotropic mechanisms in transgenic mouse model of Alzheimer's disease. FASEB J Jan 2020;34(1):1412—29. https://doi.org/10.1096/FJ.201901984R.

[27] Parcerisas A, Pujadas L, Ortega-Gascó A, Perelló-Amorós B, Viais R, Hino K, et al. NCAM2 regulates dendritic and axonal differentiation through the cytoskeletal proteins MAP2 and 14-3-3. Cerebr Cortex May 2020;30(6):3781—99. https://doi.org/10.1093/CERCOR/BHZ342.

[28] Fosch A, Rodriguez-Garcia M, Miralpeix C, Zagmutt S, Larrañaga M, Reguera AC. Central regulation of brown fat thermogenesis in response to saturated or unsaturated long-chain fatty acids. Int J Mol Sci Jan 2023;24(2). https://doi.org/10.3390/IJMS24021697.

[29] Casas M, Fadó R, Domínguez JL, Roig A, Kaku M, Chohnan S, et al. Sensing of nutrients by CPT1C controls SAC1 activity to regulate AMPA receptor trafficking. JCB (J Cell Biol) Sep 2020;219(10). https://doi.org/10.1083/JCB.201912045.

[30] Fadó R, Soto D, Miñano-Molina AJ, Pozo M, Carrasco P, Yefimenko N, et al. Novel regulation of the synthesis of α-Amino-3-hydroxy-5-methyl-4-isoxazolepropionic acid (ampa) receptor subunit glua1 by carnitine palmitoyltransferase 1C (CPT1C) in the Hippocampus. J Biol Chem Oct 2015;290(42):25548—60. https://doi.org/10.1074/jbc.M115.681064.

[31] Rothman JS, Silver RA. NeuroMatic: an integrated open-source software toolkit for acquisition, analysis and simulation of electrophysiological data. Front Neuroinf Apr. 2018;12. https://doi.org/10.3389/FNINF.2018.00014.

[32] Monday HR, Kharod SC, Yoon YJ, Singer RH, Castillo PE. Presynaptic FMRP and local protein synthesis support structural and functional plasticity of glutamatergic axon terminals. Neuron Aug. 2022;110(16):2588—2606.e6. https://doi.org/10.1016/J.NEURON.2022.05.024.

[33] Griñán-Ferré C, Codony S, Pujol E, Yang J, Leiva R, Escolano C, et al. Pharmacological inhibition of soluble epoxide hydrolase as a new therapy for alzheimer's disease. Neurotherapeutics Oct 2020;17(4):1825—35. https://doi.org/10.1007/S13311-020-00854-1.

[34] Griñan-Ferré C, Palomera-Ávalos V, Puigoriol-Illamola D, Camins A, Porquet D, Plá V, et al. Behaviour and cognitive changes correlated with hippocampal neuroinflammaging and neuronal markers in female SAMP8, a model of accelerated senescence. Exp Gerontol Jul. 2016;80:57—69. https://doi.org/10.1016/J.EXGER.2016.03.014.

[35] Youssef FF. Ketone bodies attenuate excitotoxic cell injury in the rat hippocampal slice under conditions of reduced glucose availability. Neurol Res 2015;37(3):211—6. https://doi.org/10.1179/1743132814Y.0000000430.

[36] Kimura R, Ma LY, Wu C, Turner D, Shen JX, Ellsworth K, et al. Acute exposure to the mitochondrial complex I toxin rotenone impairs synaptic long-term potentiation in rat hippocampal slices. CNS Neurosci Ther Aug. 2012;18(8):641—6. https://doi.org/10.1111/J.1755-5949.2012.00337.X.

[37] Maalouf M, Rho JM. Oxidative impairment of hippocampal long-term potentiation involves activation of protein phosphatase 2A and is prevented by ketone bodies. J Neurosci Res 2008;86(15):3322—30. https://doi.org/10.1002/JNR.21782.

[38] Nehlig A. Brain uptake and metabolism of ketone bodies in animal models. Prostaglandins Leukot Essent Fatty Acids 2004;70(3):265—75. https://doi.org/10.1016/j.plefa.2003.07.006.

[39] de León-López CAM, Carretero-Rey M, Khan ZU. AMPA receptors in synaptic plasticity, memory function, and brain diseases. Cell Mol Neurobiol Dec. 2025;45(1):14. https://doi.org/10.1007/S10571-024-01529-7.

[40] Vu T, Gugustea R, Leung LS. Long-term potentiation of the nucleus reuniens and entorhinal cortex to CA1 distal dendritic synapses in mice. Brain Struct Funct Jul. 2020;225(6):1817—38. https://doi.org/10.1007/S00429-020-02095-6.

[41] Lee HK, Barbarosie M, Kameyama K, Bear MF, Huganir RL. Regulation of distinct AMPA receptor phosphorylation sites during bidirectional synaptic plasticity. Nature Jun. 2000;405(6789):955—9. https://doi.org/10.1038/35016089.

[42] Miralpeix C, Fosch A, Casas J, Baena M, Herrero L, Serra D, et al. Hypothalamic endocannabinoids inversely correlate with the development of diet-induced obesity in male and female mice. J Lipid Res 2019;60(7):1260–9. https://doi.org/10.1194/jlr.M092742.

[43] Fosch A, Pizarro DS, Zagmutt S, Reguera AC, Batallé G, Rodríguez-García M, et al. CPT1C deficiency in SF1 neurons impairs early metabolic adaptation to dietary fats, leading to obesity. Mol Metabol 2025;96(Jun). https://doi.org/10.1016/J.MOLMET.2025.102155.

[44] Hu E, Du H, Zhu X, Wang L, Shang S, Wu X, et al. Beta-hydroxybutyrate promotes the expression of BDNF in hippocampal neurons under adequate glucose supply. Neuroscience 2018;386:315–25. https://doi.org/10.1016/j.neuroscience.2018.06.036.

[45] Jensen NJ, Wodschow HZ, Nilsson M, Rungby J. Effects of ketone bodies on brain metabolism and function in neurodegenerative diseases. Int J Mol Sci Nov. 2020;21(22):1–17. https://doi.org/10.3390/IJMS21228767.

[46] Purkey AM, Dell'Acqua ML. Phosphorylation-Dependent regulation of Ca2+-Permeable AMPA receptors during hippocampal synaptic plasticity. Front Synaptic Neurosci Mar. 2020;12. https://doi.org/10.3389/FNSYN.2020.00008.

[47] Hosokawa T, Mitsushima D, Kaneko R, Hayashi Y. Stoichiometry and phosphoisotypes of hippocampal AMPA-type glutamate receptor phosphorylation. Neuron Jan. 2015;85(1):60–7. https://doi.org/10.1016/J.NEURON.2014.11.026.

[48] Fischer T, Och U, Klawon I, Och T, Grüneberg M, Fobker M, et al. Effect of a sodium and calcium DL- β-Hydroxybutyrate salt in healthy adults. J Nutr Metab 2018. https://doi.org/10.1155/2018/9812806.

[49] Basolo A, Magno S, Santini F, Ceccarini G. Ketogenic diet and weight loss: is there an effect on energy expenditure? Nutrients May 2022;14(9). https://doi.org/10.3390/NU14091814.

[50] Muscogiuri G, El Ghoch M, Colao A, Hassapidou M, Yumuk V, Busetto L. European guidelines for obesity management in adults with a very low-calorie ketogenic diet: a systematic review and meta-analysis. Obes Facts Apr. 2021;14(2):222–45. https://doi.org/10.1159/000515381.

[51] Zhou C, Wang M, Liang J, He G, Chen N. Ketogenic diet benefits to weight loss, glycemic control, and lipid profiles in overweight patients with type 2 diabetes mellitus: a meta-analysis of randomized controlled trails. Int J Environ Res Publ Health Aug. 2022;19(16). https://doi.org/10.3390/IJERPH191610429.

[52] Lee J, Park S, Lee JY, Yeo YK, Kim JS, Lim J. Improved spatial learning and memory by perilla diet is correlated with immunoreactivities to neurofilament and α-synuclein in hilus of dentate gyrus. Proteome Sci Dec. 2012;10(1). https://doi.org/10.1186/1477-5956-10-72.

[53] Cansev M, Wurtman RJ, Sakamoto T, Ulus IH. Oral administration of circulating precursors for membrane phosphatides can promote the synthesis of new brain synapses. Alzheimer's Dement Jan. 2008;4(1). https://doi.org/10.1016/J.JALZ.2007.10.005. Suppl 1.

[54] Kavraal S, Oncu SK, Bitiktas S, Artis AS, Dolu N, Gunes T, et al. Maternal intake of Omega-3 essential fatty acids improves long term potentiation in the dentate gyrus and morris water maze performance in rats. Brain Res 2012;1482:32–9. https://doi.org/10.1016/j.brainres.2012.09.002.

[55] Yang Y, Bin Wang X, Frerking M, Zhou Q. Delivery of AMPA receptors to perisynaptic sites precedes the full expression of long-term potentiation. Proc Natl Acad Sci U S A Aug. 2008;105(32):11388–93. https://doi.org/10.1073/PNAS.0802978105.

[56] Yang Y, Bin Wang X, Zhou Q. Perisynaptic GluR2-lacking AMPA receptors control the reversibility of synaptic and spines modifications. Proc Natl Acad Sci U S A Jun. 2010;107(26):11999–2004. https://doi.org/10.1073/PNAS.0913004107.

[57] Contreras A, Oncu SK, Bitiktas S, Artis AS, Dolu N, Gunes T, et al. Inhibition of hippocampal long-term potentiation by high-fat diets: is it related to an effect of palmitic acid involving glycogen synthase kinase-3? Neuroreport 2017;28(6):354–9. https://doi.org/10.1097/WNR.0000000000000774.

[58] Hayashi T, Rumbaugh G, Huganir RL. Differential regulation of AMPA receptor subunit trafficking by palmitoylation of two distinct sites. Neuron Sep. 2005;47(5):709–23. https://doi.org/10.1016/J.NEURON.2005.06.035.

[59] Yin JX, Maalouf M, Han P, Zhao M, Gao M, Dharshaun T, et al. Ketones block amyloid entry and improve cognition in an Alzheimer's model. Neurobiol Aging 2016;39:25–37. https://doi.org/10.1016/j.neurobiolaging.2015.11.018.

[60] Blaise JH, Ruskin DN, Koranda JL, Masino SA. Effects of a ketogenic diet on hippocampal plasticity in freely moving juvenile rats. Phys Rep 2015;3(5):1–8. https://doi.org/10.14814/phy2.12411.

[61] Ramírez S, Haddad-Tóvolli R, Radosevic M, Toledo M, Pané A, Alcolea D, et al. Hypothalamic pregnenolone mediates recognition memory in the context of metabolic disorders. Cell Metab Feb. 2022;34(2):269–284.e9. https://doi.org/10.1016/J.CMET.2021.12.023.

[62] de Paula GC, Brunetta HS, Engel DF, Gaspar JM, Velloso LA, Engblom D, et al. Hippocampal function is impaired by a short-term high-fat diet in mice: increased blood–brain barrier permeability and neuroinflammation as triggering events. Front Neurosci Nov. 2021;(15). https://doi.org/10.3389/FNINS.2021.734158/PDF.

[63] Fernández-Verdejo R, Mey JT, Ravussin E. Effects of ketone bodies on energy expenditure, substrate utilization, and energy intake in humans. J Lipid Res 2023;64(10). https://doi.org/10.1016/J.JLR.2023.100442.

[64] Fu SP, Wang JF, Xue WJ, Liu HM, Liu B, Zeng YL, et al. Anti-inflammatory effects of BHBA in both in vivo and in vitro Parkinson's disease models are mediated by GPR109A-dependent mechanisms. J Neuroinflammation Jan 2015;12(1). https://doi.org/10.1186/S12974-014-0230-3.

[65] Tieu K, Perier C, Caspersen C, Teismann P, Wu DC, Yan SD, et al. D-beta-hydroxybutyrate rescues mitochondrial respiration and mitigates features of parkinson disease. J Clin Investig Sep. 2003;112(6):892–901. https://doi.org/10.1172/JCI18797.

[66] Phillips MCL. Fasting as a therapy in neurological disease. Nutrients 2019;11(10). https://doi.org/10.3390/nu11102501.

[67] Włodarek D. Role of ketogenic diets in neurodegenerative diseases (alzheimer's disease and parkinson's disease). Nutrients Jan. 2019;11(1). https://doi.org/10.3390/NU11010169.

[68] Simeone TA, Simeone KA, Rho JM. Ketone bodies as anti-seizure agents. Neurochem Res Jul. 2017;42(7):2011–8. https://doi.org/10.1007/S11064-017-2253-5.

[69] Augustin K, et al. Mechanisms of action for the medium-chain triglyceride ketogenic diet in neurological and metabolic disorders. Lancet Neurol Jan. 2018;17(1):84–93. https://doi.org/10.1016/S1474-4422(17)30408-8.

[70] Thio LL, Wong M, Yamada KA. Ketone bodies do not directly alter excitatory or inhibitory hippocampal synaptic transmission. Neurology 2000;54(2):325–31. https://doi.org/10.1212/wnl.54.2.325.

[71] Donevan SD, White HS, Anderson GD, Rho JM. Voltage-dependent block of N-Methyl-D-Aspartate receptors by the novel anticonvulsant dibenzylamine, a bioactive constituent of L-(+)-β -Hydroxybutyrate. Epilepsia Oct. 2003;44(10):1274–9. https://doi.org/10.1046/J.1528-1157.2003.07203.X.

[72] Rho JM, Anderson GD, Donevan SD, White HS. Acetoacetate, acetone, and dibenzylamine (A contaminant in L-(+)-β-hydroxybutyrate) exhibit direct anticonvulsant actions in vivo. Epilepsia 2002;43(4):358–61. https://doi.org/10.1046/J.1528-1157.2002.47901.X.

[73] Zhou T, et al. Function and mechanism of histone β-hydroxybutyrylation in health and disease. Front Immunol Sep. 2022;13. https://doi.org/10.3389/FIMMU.2022.981285.

[74] Fulghum K, Salathe SF, Davis X, Thyfault JP, Puchalska P, Crawford PA. Ketone body metabolism and cardiometabolic implications for cognitive health. Npj Metabolic Health and Disease Oct. 2024;2(1):29. https://doi.org/10.1038/S44324-024-00029-Y.

[75] Bai YP, et al. β-Hydroxybutyrate suppresses M1 macrophage polarization through β-hydroxybutyrylation of the STAT1 protein. Cell Death Dis Dec. 2024;15(12). https://doi.org/10.1038/S41419-024-07268-3.

[76] Zuo Y, et al. β-hydroxybutyrylation and O-GlcNAc modifications of STAT1 modulate antiviral defense in aging. Cell Mol Immunol 2025;22(4). https://doi.org/10.1038/S41423-025-01266-X.

